



**HAL**  
open science

# Climate and Human Evolution: Insights from Marine Records

Thibaut Caley, Antoine Souron, Kevin Uno, Gabriele A Macho

► **To cite this version:**

Thibaut Caley, Antoine Souron, Kevin Uno, Gabriele A Macho. Climate and Human Evolution: Insights from Marine Records. *Annual Review of Marine Science*, 2024, 10.1146/annurev-marine-032223-031306 . hal-04645339

**HAL Id: hal-04645339**

**<https://hal.science/hal-04645339>**

Submitted on 11 Jul 2024

**HAL** is a multi-disciplinary open access archive for the deposit and dissemination of scientific research documents, whether they are published or not. The documents may come from teaching and research institutions in France or abroad, or from public or private research centers.

L'archive ouverte pluridisciplinaire **HAL**, est destinée au dépôt et à la diffusion de documents scientifiques de niveau recherche, publiés ou non, émanant des établissements d'enseignement et de recherche français ou étrangers, des laboratoires publics ou privés.

1                                   **“Climate and Human Evolution: Insights from Marine Records”**

2                                   **Thibaut Caley<sup>1</sup>, Antoine Souron<sup>2</sup>, Kevin Uno<sup>3</sup> and Gabriele A. Macho<sup>4</sup>**

3                                   <sup>1</sup>*Univ. Bordeaux, CNRS, Bordeaux INP, EPOC, UMR 5805, F-33600 Pessac, France; email: [thibaut.caley@u-](mailto:thibaut.caley@u-bordeaux.fr)*  
4                                   *[bordeaux.fr](mailto:thibaut.caley@u-bordeaux.fr)*

5                                   <sup>2</sup>*Univ. Bordeaux, CNRS, Ministère de la Culture, PACEA, UMR 5199, F-33600 Pessac, France; email:*  
6                                   *[antoine.souron@u-bordeaux.fr](mailto:antoine.souron@u-bordeaux.fr)*

7                                   <sup>3</sup>*Department of Human Evolutionary Biology, Harvard University, Cambridge, MA, USA; email:*  
8                                   *[kevinuno@g.harvard.edu](mailto:kevinuno@g.harvard.edu)*

9                                   <sup>4</sup>*Earth and Planetary Science, Birkbeck, University of London, London WC1E 7HX, England; email:*  
10                                   *[Gabriele.A.Macho@gmail.com](mailto:Gabriele.A.Macho@gmail.com); [G.Macho@bbk.ac.uk](mailto:G.Macho@bbk.ac.uk)*

11  
12                                   **Keywords:** paleoclimate, human evolution, marine records, Africa, numerical modeling,  
13                                   causal mechanisms

14  
15                                   **Abstract:**

16                                   The relationship between climate and human evolution is complex and the causal mechanisms  
17                                   remain unknown. Here, we review and synthesize what is currently known about climate  
18                                   forcings on African landscapes, focusing mainly on the last 4Myr. We use information  
19                                   derived from marine sediment archives and data-numerical climate model comparisons and  
20                                   integration. There exists a heterogeneity in pan-African hydroclimate changes, forced by a  
21                                   combination of orbitally-paced low-latitude fluctuations in insolation, polar ice volume  
22                                   changes, tropical Sea Surface Temperature (SST) gradients, the Walker circulation and maybe  
23                                   greenhouse gases (GHGs). Pan-African vegetation changes do not follow the same pattern,  
24                                   suggestive of additional influences, such as CO<sub>2</sub> and temperature. We caution against reliance  
25                                   on temporal correlations between global or regional climate, environmental changes and  
26                                   human evolution and briefly proffer some ideas how pan-African climate trends could help  
27                                   create novel conceptual frameworks to determine the causal mechanisms between  
28                                   climate/habitat change and hominin evolution.

## 39 Introduction

40 The notion that climate influenced the course of human evolution has deep roots (Darwin  
41 1871) and has been entertained in earnest since the 1920s after the discovery of the first  
42 australopiths in southern Africa; occasional wooded belts and a relative scarcity of water were  
43 suggested to have shaped human evolution (Dart 1925).

44 Over the last few decades evolutionary hypotheses have become more formalised. For  
45 example, Vrba (1985 and subsequent publications, see 1995 for review) proposed the  
46 *turnover-pulse hypothesis*, which postulates pulses of speciation/extinctions across clades as a  
47 consequence of prolonged climatic changes, primarily at the transitions of major astronomical  
48 cycles from 19-23kyr to 41kyr, 100kyr and 400kyr respectively. Although originally  
49 conceived to explain the turnover of bovids, for which the fossil record is relatively extensive,  
50 the hypothesis was soon extended to explain major transitions in hominin evolution  
51 (deMenocal 2004). However, doubts were raised whether the hypothesis is applicable to other  
52 clades and/or across Africa (e.g., Behrensmeyer 2006). Indeed, all species are habitat-specific  
53 and although large-scale changes in habitat structure may affect a number of clades  
54 simultaneously, they will do so in different ways; this concept is encapsulated in Vrba's  
55 'habitat theory'. She argued that, exposed to the same environmental and climatic changes,  
56 warm-adapted and cold-adapted clades will display different rates and timings of species-  
57 turnover. Ecological studies have since explored the eco-evolutionary processes underlying  
58 species diversity in greater detail and have shown that, in addition to thermoregulatory  
59 constraints, a taxon's dispersal potential, dietary adaptation, body mass, life history strategy,  
60 as well as competition among species, will profoundly influence a species' response to  
61 climate change and its susceptibility to speciation/extinction (Price et al. 2012, Pires et al.  
62 2017). Hence, the association between climate change, speciation, extinction, dispersal and  
63 morphological adaptation is not straightforward and would require a multi-pronged approach  
64 for its resolution (Hagen 2023). Given the limitations of the fossil record (Behrensmeyer et al.  
65 2000), including sampling biases (Maxwell et al. 2018, Faith et al. 2021), discerning the  
66 mechanism underlying evolutionary processes in an extinct taxon is thus challenging, if not  
67 impossible. Consequently, whilst mapping hominin diversification and innovations onto  
68 global climate trends is appealing (e.g., deMenocal 2004, Figure 1) and may highlight specific  
69 time periods of interest, the explanatory power of such correlations is limited. Interpreting the  
70 effects of climate on later stages of hominin evolution is even more problematic.

71 Specifically, Potts (1995, 1996, 1998) formulated the *variability selection hypothesis*. This  
72 hypothesis is grounded in Sewall Wright's (1932, 1968) *shifting balance theory*, which  
73 mathematically explores changes in allele frequencies and genotypes in response to drift,  
74 natural selection, mutation and migration. Owing to random drift and local selection pressures  
75 some populations/species are predicted to go extinct, whilst others will traverse valleys of  
76 lower fitness to ascend to a new adaptive peak; successful species/populations are postulated  
77 to accrue certain alleles and gene configurations. Contrary to Wright however, who  
78 emphasized random shifts in gene frequencies, Potts drew attention to the role of increased  
79 climatic variability during the Pleistocene as a driver for genetic change. He suggested that  
80 habitat instability would not only have led to changes to allele frequencies, but to  
81 polymorphisms, thus making species/populations well-equipped to deal with novel situations  
82 without the need for further genetic modifications. Phrased differently, species/population  
83 would have become increasingly buffered against environmental stochasticity; increased

84 behavioural flexibility and innovations in material culture (Potts et al. 2018, 2020) would  
85 have added further advantages to the survival of hominin populations/species.

86 Evidently thus, whilst there is little doubt that hominin evolution was driven, or at least  
87 influenced, by climate change, the identification of causal mechanisms has remained elusive.  
88 In order to advance our understanding of the possible causal relationships, we need to  
89 primarily improve on two lines of enquiry: (a) obtain better (i.e. high-resolution) climate and  
90 habitat reconstructions through time and (b) develop theoretical frameworks for an  
91 interpretation of the climatic and ecological drivers for evolutionary change in a large-bodied,  
92 eurybiomic and polymorphic taxon, that has no living analog. To contribute to these aims here  
93 we will review and synthesize what is currently known about climate forcings on African  
94 landscapes, using information derived from marine sediment archives (restricted to the period  
95 from the Neogene to present day with a primary focus on the last 4Myr), data-numerical  
96 climate model comparisons and integration. The reconstruction of local environments from  
97 the terrestrial (e.g. faunal records) (e.g., Andrews & Hixson 2014) and lacustrine sedimentary  
98 archives (e.g., Campisano et al. 2017), does not form part of this review. We will then briefly  
99 proffer some ideas as to how these African climate trends could help create novel conceptual  
100 frameworks for an interpretation of hominin evolutionary processes.

101

## 102 **1. Climate forcings on African landscapes**

### 103 1.1 Natural forcings/causes of climate changes

104 Climate varies at different time scales, from years to billions of years (Figure 2). Climate  
105 variability depends on interactions between the different components of the climate system  
106 (atmosphere, ocean, cryosphere, biosphere and lithosphere) and on external forcings that  
107 affect the earth's radiative balance. External forcings are mainly related to astronomical  
108 forcings or are associated to internal Earth dynamic (Figure 2), which affect the radiative  
109 balance of the Earth and processes such as atmospheric and oceanic circulation that re-  
110 equilibrate the system by transporting excess energy from the equatorial to polar regions.  
111 Processes internal of the climate system imply different retroactions inside the system.

112 Over the last 4Myr the effects of tectonics on climate systems reduced and the main natural  
113 forcings of climate change have been related to the earth's orbital variations (eccentricity,  
114 obliquity and precession with periodicities of 100 and 400kyr, 41kyr and 21kyr, respectively)  
115 and atmosphere-ocean-cryosphere dynamics (Figure 2). Africa is centered on the equator and  
116 therefore most of its landmass is located at low latitudes where Intertropical Convergence  
117 Zone (ITCZ) variability, monsoons and Walker Circulation control the hydrological cycle.

### 118 1.2 The ITCZ, Monsoons and Walker Circulation

119 The ITCZ is a tropical belt of maximum precipitation that results from deep convection  
120 migrating seasonally towards the warming hemisphere (Nicholson et al. 2013, Schneider et al.  
121 2014). ITCZ zonal-mean position is associated with the rising branch of the global Hadley  
122 cell (Figure 3). Because of the complexity of African climate, the Congo Air Boundary  
123 (CAB), a convergence zone that marks the confluence of Indian Ocean air with unstable air  
124 from the Congo Basin, indicates the location of the southern edge of the African rain belt and

125 plays a fundamental role in controlling hydroclimate in the African tropics, especially in  
126 Africa's interior (Tierney et al. 2011, Howard & Washington 2019).

127 Monsoons are the dominant seasonal mode of climate variability in the tropics (Mohtadi et al.  
128 2016). They can be viewed as localized seasonal migrations of the tropical convergence zone:  
129 the band of converging air and rainfall in the tropics embedded within the tropical  
130 atmospheric overturning circulation. This allows to distinguish the dynamics of low-latitude  
131 ( $\sim 0\text{--}10^\circ$  poleward) ITCZ from that of monsoons ( $\sim 10\text{--}25^\circ$  poleward) (Geen et al. 2020)  
132 (Figure 3).

133 In addition to tropical convergence zone migrations, a thermally direct, equatorial, zonal  
134 overturning circulation exists that converts available potential energy to kinetic energy of  
135 atmospheric motion: the Walker Circulation. The Walker Circulation is intrinsically  
136 connected to the El Niño–Southern Oscillation (ENSO) and the Indian Ocean Dipole (IOD),  
137 which are forms of interannual climate variability in the tropical Pacific and Indian Ocean,  
138 respectively (Abram et al. 2020) (Figure 3). The results are increased/decreased atmospheric  
139 convection and associated precipitation over the western or eastern tropical Pacific and Indian  
140 Oceans.

### 141 1.3 Relationships between precipitation and vegetation changes

142 Today, the distribution of vegetation and animals in Africa is related to the amount, intensity  
143 and seasonal distribution of precipitation (e.g., White 1983, Guan et al. 2014). This  
144 connection between hydroclimate and vegetation also existed in the past and likely affected  
145 evolutionary processes. To illustrate, the vegetation and precipitation records show a marked  
146 seasonal shift across the Sahel with plant growth moving north as rain falls over the region in  
147 boreal summer (Figure 4). Conversely, plant growth moves south as rain falls over southern  
148 Africa in austral summer, although the correlation is less significant for some areas. Such  
149 heterogeneity in vegetation response is noteworthy and cautions against generalizations when  
150 reconstructing past environments. It is therefore crucial to reconstruct both past hydroclimate  
151 and vegetation changes and their potential relation in order to explore potential links with  
152 human evolution.

153

## 154 2. Interests of marine sediment records

155 deMenocal (1995) first linked early hominin evolution in Africa to global climate change,  
156 using data from marine sediment cores. Although African terrestrial records provide crucial  
157 information about land climate variability and about the specific habitats/niches occupied by  
158 extinct taxa (e.g., refugia), marine records offer a more robust chronology, a long stratigraphic  
159 continuity and higher temporal resolution (Cohen et al., 2022). A wide range of proxies can  
160 be used in marine sediment cores for terrestrial climate and environmental reconstructions  
161 (Table 1) with the advantage of direct ocean-continental comparison. For example, proxies  
162 associated with marine biogenic sedimentation can be directly compared to proxies derived  
163 from continental source that are transported, mainly by wind or rivers, to the oceans (Figure  
164 5).

165 Because marine sediments integrate the signal of entire catchments areas, reconstructing a  
166 larger picture of oceanic and atmospheric dynamics is possible. Using volcanic sediments in

167 marine sediment cores, it also becomes possible to assess more precisely the synchronicity  
168 and potential causal links between climate/environmental changes and human evolution (see  
169 **Appendices: Tectonic, volcanism and tephrochronology**).

170 With these benefits in mind, an important caveat of marine core archives is that there is a  
171 spatiotemporal scale mismatch between broad, regional marine core records and the highly  
172 localized terrestrial fossil records that inform about primate evolution (Faith et al. 2021). For  
173 example, recent biomarker isotope records from terrestrial sediments (Peppe et al. 2023, Uno  
174 et al. 2016b) and lacustrine sediments (e.g., Lupien et al. 2022, Mitsunaga et al. 2023)  
175 indicate higher ecosystem and hydroclimate variability at smaller spatial scales. In one case,  
176 carbon isotope biomarker records suggest C<sub>4</sub> vegetation at local scales that is absent in  
177 regional records (Peppe et al. 2023). Careful consideration of how marine, lacustrine, and  
178 terrestrial archives integrate vegetation and hydroclimate signals is necessary for relating  
179 proxy vegetation and climate records to hominin evolution.

180

### 181 **3. Climate and environments of Africa**

182 Given the impact of tectonics and volcanism on landscapes, building the tectonic histories of  
183 each basin should be a requisite step before linking continental records of environmental  
184 change to regional or global climate phenomena (see review in Levin 2015); most tectonic  
185 activity in Africa in the last 10Myr has centered on the East African Rift System (EARS; see  
186 **Appendices: Tectonic, volcanism and tephrochronology**). Whilst we acknowledge the  
187 importance of tectonics and volcanism for the reconstruction of local habitats, our main focus  
188 here is on pan-African climate over the last 4Myr, based on marine sediment cores, as this  
189 may have impacted the overall course of hominin evolution; to provide a broader context, we  
190 only briefly summarize marine core records that capture important climate and environmental  
191 change during the Neogene.

#### 192 **3.1 Climate and environments of the Neogene**

193 The Neogene period, which includes the Miocene (23.03 to 5.33Ma) and Pliocene (5.33 to  
194 2.58Ma) epochs, was characterized by major environmental change that influenced primate  
195 evolution in Africa. Fossils from the early and middle Miocene demonstrate a dynamic period  
196 of catarrhine evolution in Africa that includes the first *Afropithecus* and victoriapithecines and  
197 the diversification of proconsulids (Leakey & Leakey 1986, McNulty et al. 2015, Nengo et al.  
198 2017). This was followed by the origin of the hominin lineage in the late Miocene around  
199 7Ma (Brunet et al. 2002). But there is a dearth of long, continuous Neogene terrestrial  
200 archives. Most are temporally limited and associated with fossil localities in eastern Africa.  
201 As a result, marine core records have played an important role in reconstructing regional scale  
202 climate and environmental change in Africa. This includes Neogene biomarker records (Uno  
203 et al. 2016a, Polissar et al. 2019; see **Appendices: Water and Carbon isotopes**) and plant  
204 microfossil records (Morley & Richards 1993) as well as late Miocene biomarker (Feakins et  
205 al. 2013, Hoetzel et al. 2013) and pollen records (Bonnefille 2010) that span the last ~10Myr.  
206 Carbon isotope records from *n*-alkanes at DSDP sites 235 and 241 in the Somali Basin were  
207 the first to demonstrate C<sub>3</sub> vegetation was predominant at the regional scale from the early  
208 Neogene until 10Ma, when C<sub>4</sub> grasses began to spread in eastern Africa (Uno et al. 2016a).  
209 Subsequent *n*-alkane carbon isotope records from the tropical Atlantic (ODP sites 659 and

210 959) show a similar pattern of regional C<sub>4</sub> expansion in northwest Africa at 10Ma; additional  
211 hydrogen isotope records show no clear indication of hydroclimate change associated with  
212 spread of C<sub>4</sub> grasslands in Africa (Polissar et al. 2019). In southern Africa, combined  
213 biomarker, pollen, and charcoal records from ODP sites 1081 and 1085 show that grasses  
214 were present regionally by ~11Ma, with the spread of C<sub>4</sub> vegetation beginning around 7.5Ma  
215 (Hoetzel et al. 2013, Dupont et al. 2013). The Neogene marine core records from  
216 northwestern, eastern, and southern Africa demonstrate that C<sub>4</sub> grasses began to spread  
217 regionally in the northern part of the continent at 10Ma and in the southern part by 7.5Ma.  
218 Available biomarker data suggest that hydroclimate change played a minor or insignificant  
219 role and, therefore, CO<sub>2</sub> may have instead acted as the ecological driver (Polissar et al. 2019).  
220 An outstanding question that cannot be addressed by carbon isotopes is the role of C<sub>3</sub> grasses  
221 in early Neogene ecosystems, which were no doubt present based on plant microfossil  
222 evidence (Peppe et al. 2023, Morley & Richards 1993).

223

## 224 3.2 Climate and environments of the last 4Myr

### 225 3.2.1 New 4Myr-southeastern African (Limpopo) hydroclimate stack

226 Records of hydroclimate in southeastern Africa are rare over the last 4Myr, yet this is a  
227 crucial region regarding hominin evolution (Figure 1). Here we combine published  
228 hydroclimate records over the last 2Myr (Caley et al. 2018) with those between ~4 to 2Ma  
229 (Koutsodendris et al. 2021, Taylor et al., 2021) in order to generate a new Limpopo catchment  
230 hydroclimate stack over the last 4Myr (see Figure 6). We performed a principal component  
231 analysis (PCA) on the  $\delta^{13}\text{C}_{\text{wax}}$  and  $\ln(\text{Fe}/\text{Ca})$  hydroclimate records of site MD96-2048 (Caley  
232 et al. 2018) (Table 1). The first principal component (PC1) accounts, on average, for 71% of  
233 the variance. Similarly, the  $\delta\text{D}_{\text{wax}}$  and  $\ln(\text{Ti}/\text{Ca})$  hydroclimate records (Table 1) of site IODP  
234 U1478 (Koutsodendris et al. 2021, Taylor et al. 2021) accounts, on average, for 53% of the  
235 variance observed for PC1. When both PC1 are combined in a new 4Myr-southeastern  
236 African (Limpopo) hydroclimate stack (Figure 6e), significant changes with alternation  
237 between more humid and more arid conditions are evident over the last 4Myr. This finding  
238 prompted us to investigate whether the trends observed for southeastern Africa can be  
239 replicated across Africa.

### 240 3.2.2 Pan-African hydroclimate.

241 We compiled the existing continuous hydroclimate records to cover the last 4Myr. Data are  
242 limited to five records that are distributed across the whole of Africa and over several Myrs  
243 (Figure 6). Most of these records are derived from  $\delta\text{D}_{\text{wax}}$  proxy, or a combination with fluvial  
244 runoff proxies (Figure 6 and Table 1) (**Appendices: Water and Carbon isotopes**). One  
245 exception is the Dust record from site ODP659. African dust records largely reflect increased  
246 wind strength and transport (Zabel et al. 1999) however, and are not necessarily a reliable  
247 indicator for aridity (Skonieczny et al. 2019). Nonetheless, the correspondence between  $\delta\text{D}_{\text{wax}}$   
248 for specific time intervals over the last 5Myr and the dust record of ODP Site 659 apparently  
249 support conclusions concerning the generation of dust during arid periods (Tiedemann et al.  
250 1994) and the use of  $\delta\text{D}_{\text{wax}}$  as a humidity proxy (Kuechler et al. 2018).

251 To parametrize pan-African climate variability, PCA (see Figure 6 for details) of the selected  
252 datasets were performed. PC1 captures the maximum variance of the data (approximately 36

253 % across all datasets), and depicts heterogeneity across the studied sites. Hydroclimate  
254 records from the Oman region and from western Africa share a common pattern, whereas  
255 records from eastern Africa (north and more particularly south) have a different pattern.

256 To investigate the forcings that control this heterogeneity at the pan-African scale, we  
257 conducted spectral analyses. Because some of the records have a low resolution, we  
258 resampled all the datasets with a mean and regular interval of 20kyr, thereby limiting our  
259 analyses to long term orbital forcing (eccentricity scale). Spectral analyses with REDFIT  
260 (Schulz & Mudelsee 2002) and wavelet analyses (Torrence & Compo 1998) display strong  
261 spectral power at around the 185, 400 and 600kyr bands on PC1 (Figure 6). This corresponds  
262 to eccentricity forcing at 400kyr and, potentially, to weak but real eccentricity variations at  
263 around 200 and 600kyr (Kashiwaya et al. 2001, Laskar et al. 2004, Hilgen et al. 2020).  
264 Alternatively, harmonic of the 400-kyr cycle or “double” ~100-kyr cycle that result from non-  
265 linear responses of the climate system to the main eccentricity components can also explain  
266 these cycles (Hilgen et al. 2015).

267 The 400kyr and 600kyr band comprises 11 % of the variance of the PC1. Part of the variance  
268 related to orbital forcing is missing due to sampling resolution: for example, the precession  
269 forcing in south-east Africa over the last 2.15Myr accounts for 25 % of the variance in the  
270 lnFe/Ca record, a high-resolution proxy of fluvial runoff (Caley et al. 2018). Nevertheless, the  
271 results indicate that part of the variance in pan-African hydroclimate records is not controlled  
272 by orbital forcings. These other forcings have been highlighted in various studies and may  
273 relate to ice volume changes, SST gradients and the Walker circulation (Maslin et al. 2014,  
274 Caley et al. 2018, Kaboth-Bahr et al. 2021, Trauth et al. 2021, Lupien et al. 2023, Rubbelke et  
275 al. 2023), or perhaps greenhouse gases (GHGs). Although not yet fully explored, GHGs  
276 forcing could affect the hydroclimate through vegetation changes (Dupont et al. 2019) or  
277 through thermodynamic impacts, as well as consequent changes in atmospheric moisture  
278 content, resulting in summer monsoon precipitation change overall.

279  
280 When the dominant 400kyr and 600kyr cycles are removed from PC1, the residual trend  
281 correlates with gradual Walker circulation changes, ice volume changes and, to a lesser  
282 degree, CO<sub>2</sub> concentration changes (Figure 7), confirming that all of these internal forcings  
283 (Figure 2 and 7) probably affect pan-African hydroclimate variability.

284 The reconstructed pan-African climate variability, represented by PC1, clearly depicts four  
285 phases during the last 4Myr that have been constrained by change point analysis (Figure 6).  
286 The first phase characterizes a pan-African climate that is rather humid between 4 and  
287 2.51Ma. Only eastern African records indicate successions of arid and humid periods inside  
288 this first phase (see Figures 6 and 8). A second phase from 2.51 to 0.95Ma shows a gradual  
289 drying trend, except for eastern Africa, where a humid trend is observed. This period can be  
290 subdivided into two intervals (before and after 1.57Ma) where various hydroclimate trends are  
291 observed, in particular in eastern Africa. A third phase of global African aridity between 950  
292 ka to present day is characterized by a tendency toward slightly more humid conditions from  
293 around 400 ka to the present.

294 The major and gradual drying trend, together with the different patterns observed between  
295 eastern Africa and western Africa and Oman during phase 2, has been suggested to be the results  
296 of the synchronous development of the Indo-Pacific Walker cells at around 2.2-2Ma (Figure 7,  
297 Van der Lubbe et al. 2021). The long-term enhancement of the Walker circulation would have



298 suppressed (convective) rainfall in eastern Africa (Van der Lubbe et al. 2021) and would have  
299 extended well beyond eastern Africa. Indeed, recent synthesis of terrestrial and marine proxy  
300 records over the last 620kyr found a tight correlation between moisture availability across  
301 Africa and the manifestation of the Walker Circulation driving opposing wet–dry states in  
302 eastern and western Africa with influence on early modern humans by increasing resource-rich  
303 and stable ecotonal settings (Kaboth-Bahr et al. 2021). In addition, we observe a significant  
304 correlation between northern hemisphere ice-sheets expansion, decrease in CO<sub>2</sub> concentration  
305 and pan-African hydroclimate change.

306 Changes in CO<sub>2</sub> levels are important, as they will mediate vegetation changes (Dupont et al.  
307 2019). This makes the use of vegetation proxies in marine sediment cores as hydroclimate  
308 proxies more complicated. Indeed, Dupont et al. (2019) found the vegetation of the Limpopo  
309 River catchment and the coastal region of southern Mozambique not only influenced by  
310 hydroclimate but also by temperature and atmospheric CO<sub>2</sub>. In northwestern Africa, increases  
311 in precipitation were shown to be associated with an expansion of grasslands into desert  
312 landscapes, whereas changes in CO<sub>2</sub> predominantly drove the C<sub>3</sub>/C<sub>4</sub> composition of savanna  
313 ecosystems over the last ~500kyr (O'Mara et al. 2022). On longer time scales, although  
314 debated (Schefuß & Dupont 2020), Polissar et al. (2019) suggested that C<sub>4</sub>-dominated  
315 ecosystems expanded synchronously across northwestern and eastern Africa after 10Ma  
316 without substantial changes in palaeohydrology but coincident with latitudinal temperature  
317 changes and declining atmospheric CO<sub>2</sub>. Taken together therefore, the interactions between  
318 hydrology and CO<sub>2</sub> concentration in deep time are not entirely clear and require further  
319 investigation. This lack of understanding also impacts our reconstruction of past vegetation,  
320 although this can be partly overcome by analyses of marine cores.

### 321 3.2.3 Pan-African vegetation.

322 Our compilation of vegetation data over the last 4 Myr support a synchronous expansion of  
323 C<sub>4</sub>-dominated ecosystems across northern, southwestern, and eastern Africa after 4 Ma, with  
324 more stable conditions at around 1Ma (Figure 9) (**Appendices: Water and Carbon**  
325 **isotopes**). This synchronicity of pan-African vegetation changes seems to contrast with what  
326 is observed in terms of pan-African hydroclimate changes (Figures 6 and 8), although  
327 vegetation records over the last 4Myr in southeastern Africa are missing to conclusively  
328 establish this difference.

329 To further test the relationship between hydroclimate and vegetation, we explored the  
330 correlations between these two measures at site ODP1081 (southwestern Africa) and 966-967  
331 (northeastern Africa). For vegetation, we used the biomass proxy ( $\delta^{13}\text{C}_{\text{wax}}$ ) and plant  
332 reproduction proxy (desert pollen) in comparison to  $\delta\text{D}_p$ , a hydroclimate proxy. Analyses  
333 reveal a statistically significant, but weak, linear correlation ( $R = -0.54, -0.4$  or  $0.27$ ) between  
334 vegetation and hydroclimate changes, suggesting additional controls on vegetation other than  
335 hydroclimate, although some biases in proxies are also possible (Table 1).

336

## 337 4. Data comparison and integration with numerical climate models

338 4.1 Piecing together the puzzle: extrapolating from incomplete records to a more complete  
339 picture

340 Owing to the limited data available relating to the environment and climate of the regions of  
341 palaeoanthropological interest, and because of the limitations of the fossil record (e.g.,  
342 Maxwell et al. 2018, Faith et al. 2021), it has remained challenging to establish links between  
343 climate shifts and human evolution and alternative approaches have been sought: modeling.

344 For example, Eriksson et al. (2012) used numerical climate simulations to estimate  
345 temperature, precipitation and primary productivity over the past 120kyr to model  
346 demographic changes and dispersals of human populations. Although they did not use any  
347 archaeological and anthropological data to validate the model, the estimated arrival times of  
348 humans on different continents predicted by the model are broadly consistent with the fossil  
349 and archaeological record. Similarly, spatiotemporal estimates of climate and sea level  
350 changes were calculated from orbital-scale global climate swings to infer human dispersals  
351 and late Pleistocene global population distributions (Timmermann & Friedrich 2016). Indeed,  
352 modeling approaches have become increasingly popular over the last few years. By using  
353 numerical climate models and their equilibrium or transient simulations, and by drawing on  
354 the paleontological/archaeological record, researchers have attempted to identify the  
355 spatiotemporal habitat suitability of hominin species (d’Errico et al. 2017, Gibert et al. 2022,  
356 Timmermann et al. 2022, Ruan et al. 2023, Zeller et al. 2023, Ao et al. 2024). To capture  
357 important topographic barriers, which may have affected the dispersal and distribution of  
358 archaic humans, topographic downscaling is realized in some studies. When determining the  
359 spatiotemporal habitat suitability of a hominin taxon, a set of climatic variables (precipitation,  
360 temperature and net primary productivity) is simulated with numerical climate models and a  
361 climatic envelope is created for specific taxa, based on the known distribution of hominin  
362 occurrences (Timmermann et al. 2022, Gibert et al. 2022) (Figure 10); these geographic areas  
363 are then assumed to represent the fundamental niche of that hominin (Soberón & Nakamura  
364 2009).

#### 365 4.2 How trustworthy are these models?

366 To support numerical climate transient simulations, evaluations of the ability of these models  
367 to reproduce key paleoclimate records are required. For example, Timmermann et al. (2022)  
368 conducted a global data-model comparison and found “close agreement”. Our new  
369 hydroclimate compilation (Figure 6) allows further testing of that model. We focus on  
370 precipitation, because, of the four climatic variables used to produce a climatic envelope  
371 model by Timmermann et al. (2022), three are related to precipitation. Data-model  
372 comparisons highlight some disagreements between the reconstructed and the modeled  
373 precipitation for some regions of Africa in terms of general trends and variability (the  
374 correlations are weak, but statistically significant nonetheless, Figure 11). Better concordance  
375 is found for the last 1Myr compared to the entire 3Myr record, but these correlations remain  
376 weak. These discrepancies could be the result of inherent uncertainties associated with the  
377 proxies to reconstruct the precipitation changes (Table 1) (**Appendices: Water and Carbon  
378 isotopes**), biases in model simulation, such as inappropriate insolation forcing, constant last  
379 glacial maximum ocean bathymetry and land-sea mask (Yun et al. 2023), and/or potential  
380 biases in the applied ice-sheets and GHGs forcings. Either way, any conclusions drawn from  
381 these models for evolutionary purposes are thus rendered speculative. Higher resolution data,  
382 more simulations with various models and better constraints and downscaling approaches are  
383 therefore necessary.

384 In addition, to bridge paleoclimate data and models, different innovations and improvements  
385 should be considered. For example, chemical tracers (e.g., water or carbon isotopes,  
386 **Appendices: Water and Carbon isotopes**), which are relevant climate proxies, should be  
387 input directly into Earth system models. Paleoclimate information could thus be used to  
388 directly constrain model performance (“apples-to-apples” comparison). Furthermore,  
389 simulations of climate and its associated isotopic signal into models provide a “transfer  
390 function” between isotopic signal and the considered climate variables (Sturm et al. 2010,  
391 Caley et al. 2014, Collins et al. 2017).

392 A further improvement on existing models would be to combine proxy data and climate  
393 model simulations in a mathematical framework to improve insights derived from either  
394 resource independently. Data assimilation techniques have recently been adapted for  
395 paleoclimate applications (Hakim et al. 2013, Tierney et al. 2020a), resulting in spatially  
396 complete reconstructions of multiple climate variables. A balance between proxy information  
397 and the physics and covariance structure of the climate model can thus be achieved (Tierney  
398 et al. 2020b). As more high resolution and well-dated paleoclimatic records become available,  
399 and as computing power increases, data assimilation techniques could be realized over periods  
400 spanning millions of years and the outcomes could be used to force different models. Only  
401 then will we possibly be able to demonstrate an unequivocal link between climate change and  
402 human evolution from modelling approaches. Until then, we need to draw on established  
403 biological and ecological principles to discern patterns in human evolution that could perhaps  
404 be linked to global climatic and environmental changes.

405

## 406 **5. Hominin evolutionary processes and climate**

407 Over the past several decades researchers have expanded the hominin fossil record and have  
408 assembled more detailed late Cenozoic paleoclimatic, paleoenvironmental and  
409 paleoecological archives, both at the global (this contribution) and the local scale (e.g.,  
410 Campisano et al. 2017, Potts et al. 2018.). Moreover, much effort has been expended to  
411 document changes in mammalian community structure through time (e.g., Bobe et al. 2002,  
412 Werdelin & Lewis 2005) with the aim to identify turnover pulses (Vrba 1995, but see Bibi &  
413 Kiessling 2015) and/or changes in the functional composition of communities as a proxy of  
414 past climates and vegetation structures (e.g., Reed 1997, Andrews & O’Brien 2000, Hempson  
415 et al. 2015, Rowan et al. 2016, Robinson et al. 2017). Yet, the climatic and environmental  
416 drivers underpinning hominin diversity, extinction/speciation, morphological adaptations and  
417 dispersals remain elusive. In part, this may be due to the limitations of the hominin fossil  
418 record (Faith et al. 2021), taphonomic bias (e.g., Behrensmeyer et al. 2000) and differential  
419 research efforts across the continent (e.g., Maxwell et al. 2018). Perhaps the biggest obstacle  
420 of relating climate to specific processes in hominin evolution however is our unique  
421 evolutionary path towards becoming increasingly eurybiomic.

422 As early as 3.4-2.9Ma *Australopithecus afarensis* was apparently able to cope with substantial  
423 environmental variability, both with regard to biome structure and temperature (Bonnefille et  
424 al. 2004). In fact, an increase in the prevalence of C<sub>4</sub> biomass on the landscape (Figures 9 and  
425 10) is accompanied by an increase in C<sub>4</sub>-based food consumption across all hominin taxa,  
426 except in *A. sediba* (Figure 12). (**Appendices: Water and Carbon isotopes**). This is  
427 particularly evident in hominins from South Africa, a region that exhibited higher

428 hydroclimate variability over the last 4 Myr than northeastern Africa (Figures 6 and 11).  
429 However, the supposed ‘broadened dietary niche’ of South African hominins (like in *A.*  
430 *afarensis*) may simply reflect the species’ dietary flexibility through precession-led biome  
431 changes, i.e. their ability to adapt to local conditions (Hopley & Maslin 2010). Even where  
432 hominins are apparently specialized in their dietary adaptations, as in the case of  
433 *Paranthropus boisei*, detailed analyses of the nutritional components of the possible diet  
434 implies that they were nonetheless eclectic feeders (Macho 2014a) as well as habitat  
435 generalists (Patterson et al. 2022, Wood & Strait 2004, but see O’Brien et al. 2023).  
436 *Paranthropus boisei* demise may thus not be directly related to climate and vegetation  
437 change, but to other factors which may, of course, be indirectly related to climate and habitat  
438 changes, e.g. increased competition and predation risk due to habitat fragmentation. Only for  
439 *A. bahrelghazali* exists a possible link between morphological constraints on masticatory  
440 capabilities and the deterioration in palaeoenvironmental conditions, which may have  
441 triggered demographic changes and, ultimately, species’ extinction (Macho 2015); due to  
442 limited sample sizes this suggestion is likely to remain theoretical however. In southeastern  
443 Africa, local terrestrial ecosystems were impacted by long-term aridification and extreme  
444 precessional hydroclimate variability between around 1 and 0.6 Ma (Caley et al. 2018). It is  
445 intriguing (and perhaps no coincidence) that the new Limpopo hydroclimate stack matches  
446 the presence of *P. robustus* with the more humid climate trend observed over the last 4Myr  
447 (Figures 1 and 6) and may point towards a particular niche adaptation in *P. robustus* (Caley et  
448 al. 2018), a suggestion which needs to be explored further in the future.

449 With the emergence of *Homo*, habitat tolerances increased even further, aided by material  
450 culture (Potts et al. 2018, 2020). This makes it impossible to define *Homo*’s fundamental (as  
451 opposed to the realized) niche, unless it can be unequivocally demonstrated that there exists  
452 (or existed) a narrow constraint on the genus’ physiology with regard to thermoregulation,  
453 diet, photoperiodicity (i.e. life history) etc. (Soberón & Nakamura 2009). It seems  
454 improbable, however, that these traits are/were narrowly defined within any of the *Homo*  
455 species. Hence, we remain cautious about overinterpreting the outcomes of modeling studies  
456 that apply ecological niche modeling to the distribution of *Homo* (Timmermann et al. 2022,  
457 Ruan et al. 2023, Zeller et al. 2023). *Homo* species may have had habitat preferences, but it is  
458 unclear whether they were confined to these habitats (sampling biases aside). Regardless,  
459 these models are useful for a number of purposes: (a) to identify potential dispersal corridors,  
460 e.g. from the coastal regions to the African interior during the Plio-Pleistocene (Joordens et al.  
461 2019) or from Africa to Eurasia (Ao et al. 2024) or/and (b) to document how, when and where  
462 habitats became fragmented, particularly within Africa during the Plio-Pleistocene; this will  
463 aide our understanding of hominin dispersals within Africa, e.g. between western and eastern  
464 Africa (Kaboth-Bahr et al. 2021) and when local populations may have become fragmented  
465 and isolated (i.e. vicariance).

466  
467 For example, model results suggest that, during the mid-to-late Pliocene (4–3Ma), southern  
468 and eastern African hominins were separated by an environmental barrier which could only be  
469 crossed during particular periods, such as northern hemisphere summer at perihelion (Gibert  
470 et al. 2022). Arguably, this would have influenced the evolutionary pathways -and/or  
471 divergence?- of hominins. On a more local scale, Maslin et al. (2014) formulated the *pulsed*  
472 *climate variability hypothesis*, which considers inter-basin connections to be periodically  
473 disrupted by extreme wet–dry cycles. These disruptions, in turn, could have led to hominin  
474 isolation, speciation/extinctions and dispersal. A similar mechanism was invoked to explain

475 the high morphological variability in South African *Australopithecus africanus*: as the habitat  
476 periodically expanded and contracted (e.g., orbital forcing), peripheral populations may have  
477 become isolated only to fuse again when environmental conditions permitted (Brain 1985).  
478 The biological implications of such dynamic changes in habitat structure (and size) are three-  
479 fold: (i.) small populations/species with restricted habitat sizes are faced with high extinction  
480 risks as they become demographically unviable (Macho 2014b); (ii.) inevitably, genetic drift  
481 will occur (chance) and selective pressures acting on these sub-populations will either  
482 eliminate (extinction) or speed up evolutionary changes; and (iii.) the subsequent merging of  
483 temporarily separated populations may lead to the mixing of genes and the emergence of  
484 novelty (Scerri et al. 2019, van Holstein & Foley 2022), as demonstrated for baboons, for  
485 example (Sithaldeen et al. 2015, Sørensen et al. 2023).

486 In summary therefore, insights obtained from proxy, model, and combined proxy-model  
487 climate reconstructions are crucial for an understanding of hominin evolutionary processes,  
488 but to draw conclusions is complex. Early humans have no living analog for comparison and  
489 they are unique amongst primates in the way in which they have expanded their ecological  
490 niche over the last 4Myr. Whilst it is tempting to look for commonalities in species turnover  
491 across clades, we believe that clade-specific traits need to be considered in any such  
492 comparison (*sensu* Vrba, 1995). This is important if we wish to identify the causal  
493 mechanisms between climate/habitat change and hominin evolution. Correlation does not  
494 mean causation.

495

## 496 **Appendices:**

### 497 1. Tectonic, volcanism and tephrochronology:

498 The African plate is fragmenting in its eastern part, along an axis that forms the East African  
499 rift (East African Rift System: EARS). Most tectonic activity in Africa in the last 10Myr has  
500 centered on the EARS. Paleo-modeling studies have shown that uplift of the African plateau  
501 led to a drastic reorganization of atmospheric circulation, engendering strong aridification and  
502 paleoenvironmental changes, in part reflecting the setting of present-day vegetation patch  
503 work in Africa (e.g., Sepulchre et al. 2006, Munday et al. 2023).

504 Southern Africa was subject to some moderate uplift (Dirks & Berger 2013) that resulted in  
505 dynamic, high-relief landscapes (e.g., Moore et al. 2009, Bailey et al. 2011). The main uplift  
506 occurred during Oligocene (30Ma, Burke & Gunnell 2008), early-mid Miocene (15Ma), and  
507 Pliocene-Early Pleistocene (5–2Ma; Partridge, 1998), the latter probably reflecting the  
508 southward propagation of the EARS (Hartnady & Partridge 1995).

509 Rifting on the EARS started at the end of the Oligocene (WoldeGabriel et al. 1990), with  
510 clear indications of rifting by 15–10Ma (McDougall & Brown 2009, Roberts et al. 2012).  
511 During the Quaternary, this rifting would have been facilitated by the propagation of faults  
512 linked to the presence of large felsic volcanic centers (Abebe et al. 2007). This coincides with  
513 the surface manifestation of a hot spot, responsible for the emission of Ethiopian trapps  
514 around 30Ma, a considerable volume (at least  $1.2 \times 10^6 \text{ km}^3$ , Rochette et al. 1998) of basalt  
515 effusions (Courtillet et al. 2003) distributed today between Yemen and Ethiopia.

516 Volcanism in the central sector of the Ethiopian rift also began in the Oligocene and can be  
517 grouped into six episodes (WoldeGabriel et al. 1990). In the Pliocene, voluminous ignimbrites  
518 (e.g. Butajira ignimbrite, > 250 m thick) were described and correlated with tephras from the  
519 Gulf of Aden (WoldeGabriel et al. 1992). Abebe et al. (2007) recognized two episodes of  
520 activity in the Quaternary: between 2 and 1 Ma and since 650 ka. This last volcanic episode is  
521 associated with large calderas (e.g. Corbetti: 20 x 15 km; Shala: 20 x 18 km; Hutchison et al.  
522 2016).

523 The fill of the Ethiopian rift is dominated by volcano-clastic and fluvio-lacustrine sediments  
524 drained by the Awash and Omo rivers. These are mostly fluvio-deltaic deposits, within which  
525 numerous volcanic tuffs are interspersed (at least 130 recorded around Lake Turkana, Brown  
526 et al. 1992). Within these sedimentary formations, numerous hominin fossils and stone tools  
527 were found (e.g. White et al. 2003, Niespolo et al. 2021, Delagnes et al., 2023).

528 Given the presence of numerous volcanic tuffs in the region, most fossils and artifacts are  
529 dated based on their stratigraphic position relative to these tuffs. The latter can be dated if  
530 they contain sanidine crystals using potassium-argon (K-Ar) method or argon-argon (Ar-Ar)  
531 methods. However, some tuffs are impossible to date. For most of the others, the stratigraphic  
532 position and the correlations together with ages, uncertainties of the tuffs dating are a matter  
533 of debate (Brown et al. 2012, Sahle et al. 2019, Vidal et al., 2022). These led some authors to  
534 look for volcanic layers, tephras or cryptotephras in the oceanic domain (Gulf of Aden,  
535 Arabian sea), where it is then possible to apply other dating methods (e. g. Brown et al. 1992,  
536 deMenocal & Brown 1999).

537  
538 By transferring the marine chronology to continental tuffs, uncertainties in dating can be  
539 reduced. Uncertainties with benthic isotope stratigraphy of the LR04 age model (Lisieski &  
540 Raymo 2005) are 30kyr from 5–4 Ma, 15kyr from 4–3Ma, 6kyr from 3–1Ma, and 4kyr from  
541 1–0Ma; they are lower than most of the continental tuffs ages, in particular for the last 3Myr  
542 (Roberts et al. 2021, Vidal et al., 2022). The majority of tephras and cryptotephras in marine  
543 sediment cores have been found between ca. 4Ma and 0.75Ma (Sarna-Wojcicki et al. 1985,  
544 Brown et al. 1992, deMenocal & Brown 1999, Feakins et al. 2007) but more could be  
545 discovered in the future to improve chronologies (Albaredes et al. 2023).

546

## 547 2. Water and Carbon isotopes

### 548 Water isotopes

549 Water isotopes are excellent tracers of the hydrological cycle (e.g., Craig & Gordon 1965, Gat  
550 1996). Because of small chemical and physical differences between the main isotopic forms  
551 of the water molecule ( $\text{H}_2^{16}\text{O}$ , HDO,  $\text{H}_2^{18}\text{O}$ ), an isotopic fractionation occurs, principally  
552 during phase transitions of water (evaporation and condensation processes). Stable water  
553 isotopes have therefore been measured in a large variety of archives to reconstruct regional  
554 climate variations.

555 Water isotopes are expressed in per mil (‰) using  $\delta$  notation:  $\delta\text{D}$  or  $\delta^{18}\text{O} = (\text{R}_{\text{sample}} - \text{R}_{\text{standard}}) /$   
556  $\text{R}_{\text{standard}} * 1000$  and represent the relative deviation of R (the isotope ratio, D/H or  $^{18}\text{O}/^{16}\text{O}$ ) in  
557 the sample from a standard, usually Vienna Standard Mean Ocean Water (VSMOW) with  $\delta\text{D}$   
558 or  $\delta^{18}\text{O} = 0$  ‰.

559 The cuticular wax layers of higher terrestrial plant leaves contain large amounts of long-chain  
560 n-alkanes, n-alcohols, n-alkanoic acids, which are well preserved in the sedimentary record  
561 over geological timescales (Sachse et al. 2012). As water is the primary hydrogen source of  
562 photosynthesizing organisms and their biosynthetic products organic hydrogen preserved in  
563 sediments may record the isotopic composition of water used during photosynthesis and could  
564 be used as a paleohydrological proxy (Sternberg 1988). The  $\delta D_{wax}$  proxy has been  
565 increasingly used over the past decades in paleoclimate studies of marine sediment cores (e.g.  
566 Schefuß et al. 2005, Collins et al. 2017, Kuechler et al. 2013, Tierney et al. 2017, Caley et al.  
567 2018) to infer indirect changes in the regional hydrological cycle across Africa. Although the  
568  $\delta D_{wax}$  is commonly interpreted as a proxy for the amount of regional rainfall, interpretation  
569 can be more complex, because the  $\delta D_p$  value depends on other climate influences  
570 (precipitation, temperature, source effect, circulation regime) and on additional environmental  
571 and physiological processes related to the climate and the vegetation (relative humidity,  
572 vegetation changes, biosynthesis of the lipids) (Sachse et al. 2012).

573 In marine sediment cores, the seawater oxygen isotope composition ( $\delta^{18}O_{sw}$ ) is preserved in  
574 carbonates from various organisms such as foraminifers. The carbonate isotopic concentration  
575 ( $\delta^{18}O_c$ ) is mainly controlled by the temperature dependence of the equilibrium fractionation of  
576 calcite precipitation and by the isotopic composition of seawater in which the shell grew  
577 (Urey 1947, Shackleton 1974). For benthic foraminifera, it has long been assumed that the  
578 deep temperature effect on  $\delta^{18}O_c$  is negligible. Therefore, benthic  $\delta^{18}O_c$  records and stack  
579 (LR04, Lisieski & Raymo 2005) have been used to document polar ice volume changes and  
580 associated glacial/interglacial periods given that the waning and waxing of ice-sheets control  
581 the global  $\delta^{18}O_{sw}$  changes. Recent studies indicate that significant changes in deep ocean  
582 temperature exist (Elderfield et al. 2012, Sosdian & Rosenthal 2009) and that this can create  
583 large temporal offset during the onset of the Plio-Pleistocene ice ages (Rohling et al. 2014),  
584 for example between a marked cooling step at 2.73Ma and the first major glaciation at 2.15  
585 Ma. Hence,  $\delta^{18}O_{sw}$  is better suited as a proxy for polar ice volume changes rather than the  
586 benthic  $\delta^{18}O_c$  signal (Figure 7) (Rohling et al. 2021). In addition, a vast majority of marine  
587 sediment cores have age models based on stratigraphic alignment of the  $\delta^{18}O_c$  of benthic  
588 foraminifera, which measures changes in ice volume and deep ocean temperature. The use of  
589 a single global alignment target (LR04  $\delta^{18}O_c$  global stack) neglects regional differences of  
590 several thousand years in the timing of benthic  $\delta^{18}O$  change during glacial terminations.  
591 Regional  $\delta^{18}O_c$  stacks have therefore been proposed and offer better stratigraphic alignment  
592 targets although they are currently limited to the last 150kyr (Lisieski & Stern 2016).

### 593 Carbon isotopes

594 Carbon isotopes are expressed in per mil (‰) using  $\delta$  notation:  $\delta^{13}C = (R_{sample} - R_{standard}) /$   
595  $R_{standard} * 1000$  and represents the relative deviation of R (the isotope ratio,  $^{13}C/^{12}C$ ) in the  
596 sample from a standard (usually Vienna Pee Dee Belemnite (VPDB), a marine carbonate).  
597  $\delta^{13}C$  is used as a proxy for the proportion of  $C_3$  and  $C_4$  vegetation preserved in soil  
598 carbonates, fossil teeth, and leaf waxes. For reviews of how carbon stable isotopes are used to  
599 reconstruct hominin paleoenvironments see Cerling (2014) and Levin (2015). Some recent  
600 studies (e.g., Blondel et al. 2018, Souron 2018 and references herein) point out that  
601 interpretations of carbon isotopes as paleodiets are not that straightforward and should also  
602 consider independent proxies (e.g., morphology, dental microwear and mesowear) that are  
603 more directly linked to mechanical properties of diet items.

604 **Summary points:**

605 - Although African terrestrial records provide crucial information on land climate variability,  
606 marine records offer the possibility of more robust chronology, a stratigraphic continuity with  
607 a high temporal resolution and the advantage of direct ocean-continental comparison. By  
608 transferring the marine chronology to continental tuffs, a global coherent framework with  
609 hominin fossils, artefacts, climate and environmental changes can be established.

610 - A heterogeneity for pan-African hydroclimate changes is observed over the last 4Myr. The  
611 forcings that control this heterogeneity of variability are a combination of orbitally paced low-  
612 latitude fluctuations in insolation, polar ice volume changes, tropical SST gradients and the  
613 walker circulation and maybe GHGs changes.

614 - Our compilation of vegetation data over the last 4Myr show an expansion of the C<sub>4</sub>-  
615 dominated ecosystems across northern, southwestern, and eastern Africa over the last 4Myr  
616 with more stable conditions at around 1Ma, but this is not mirrored by the observed pan-  
617 African hydroclimate changes. This may indicate that the feed-back loops between climate  
618 and vegetation are more complex, whereby vegetation changes likely reflect a combination of  
619 factors including atmospheric CO<sub>2</sub> concentrations and temperature.

620 - Although temporal correlations between global or regional climate, environmental changes  
621 and human evolution can be observed over the last 4Myr, we raise some concerns as to  
622 whether these correlations reflect causal processes. We highlight a few areas where we  
623 believe that focused research effort would be warranted.

624 - We advocate that more numerical transient simulations with various climate models and  
625 better constraints and downscaling approaches should be conducted in order to assess the  
626 range of model responses and the robustness of the mechanisms leading to the simulated  
627 climate changes. To bridge paleoclimate data and models, the inclusion of chemical tracers  
628 (for example water and carbon isotopes, forward proxy modelling) relevant to proxies directly  
629 in Earth system models should be considered. Data assimilation techniques adapted for  
630 paleoclimate applications may further improve reconstructions of past climates.

631

632 **DISCLOSURE STATEMENT**

633 The authors are not aware of any affiliations, memberships, funding, or financial holdings that  
634 might be perceived as affecting the objectivity of this review.

635 **ACKNOWLEDGMENTS**

636 T.C. is grateful to Thomas Extier for help with vegetation (NDVI) data and Hugo Albaredes  
637 for discussion on volcanism and tephrochronology. We are grateful to Gauthier Devilder for  
638 his beautiful work on Figure 1 and the *carcadé* break times. T.C. is supported by CNRS Terre  
639 & Univers. This research was supported by the ANR HYDRATE project, grant ANR-21-  
640 CE01-0001 of the French Agence Nationale de la Recherche and received financial support  
641 from the French government in the framework of the University of Bordeaux's IdEx  
642 "Investments for the Future" program / GPR "Human Past".

643



644 **LITERATURE CITED**

- 645 Abebe B, Acocella V, Korme T, Ayalew D. 2007. Quaternary faulting and volcanism in the  
646 Main Ethiopian Rift. *J. Afr. Earth Sci.* 48:115–124
- 647 Abram NJ, Hargreaves JA, Wright NM, Thirumalai K., Ummenhofer CC, England MH. 2020.  
648 Palaeoclimate perspectives on the Indian Ocean dipole. *Quat. Sci. Rev.* 237:106302  
649
- 650 Albaredes H, Ducassou E, Caley T, Souron A. 2023. Cryptotephra offshore the Main  
651 Ethiopian Rift and their potential to date hominin fossils. [https://rst2023-](https://rst2023-rennes.sciencesconf.org/484446)  
652 [rennes.sciencesconf.org/484446](https://rst2023-rennes.sciencesconf.org/484446) (Abstr.)  
653
- 654 Andrews P, O'Brien EM. 2000. Climate, vegetation, and predictable gradients in mammal  
655 species richness in southern Africa. *J. Zool.* 251:205–23
- 656 Andrews P, Hixson S. 2014. Taxon-free methods of palaeoecology. *Ann. Zool. Fennici* 51:  
657 269–284  
658
- 659 Ao H, Ruan J, Martínón-Torres M, Krapp M, Liebrand D, et al. 2024. Concurrent Asian  
660 monsoon strengthening and early modern human dispersal to East Asia during the last  
661 interglacial. *PNAS* 121:e2308994121
- 662 Bailey GN, Reynolds SC, King GCP. 2011. Landscapes of human evolution: models and  
663 methods of tectonic geomorphology and the reconstruction of hominin landscapes. *J. Hum.*  
664 *Evol.* 60:257–280
- 665 Bard E. 2022. *Évolution du climat et de l'océan: Leçon inaugurale prononcée au Collège de*  
666 *France le jeudi 7 novembre 2002.* Collège de France
- 667 Behrensmeier AK. 2006. Climate change and human evolution. *Science* 311:476–478  
668
- 669 Behrensmeier AK, Kidwell SM, Gastaldo RA. 2000. Taphonomy and paleobiology.  
670 *Paleobiology* 26:103–147  
671
- 672 Beyene Y, Katoh S, WoldeGabriel G, Hart WK, Uto K, et al. 2013. The characteristics and  
673 chronology of the earliest Acheulean at Konso, Ethiopia. *PNAS* 110:1584–1591  
674
- 675 Bibi F, Kiessling. 2015. Continuous evolutionary change in Plio-Pleistocene mammals of  
676 eastern Africa. *PNAS* 112:10623–10628  
677
- 678 Blondel C, Rowan J, Merceron G, Bibi F, Negash E, et al. 2018. Feeding ecology of  
679 Tragelaphini (Bovidae) from the Shungura Formation, Omo Valley, Ethiopia: contribution of  
680 dental wear analyses. *Palaeogeogr. Palaeoclimatol. Palaeoecol.* 496:103–120  
681
- 682 Bobe R, Behrensmeier AK, Chapman RE. 2002. Faunal change, environmental variability  
683 and late Pliocene hominin evolution. *J. Hum. Evol.* 42:475–497  
684
- 685 Bonnefille R. 2010. Cenozoic vegetation, climate changes and hominid evolution in tropical  
686 Africa. *Glob. Planet. Change* 72:390–411  
687
- 688 Bonnefille R, Potts R, Chalié F, Jolly D, Peyron O. 2004. High-resolution vegetation and  
689 climate change associated with Pliocene *Australopithecus afarensis*. *PNAS* 101:12125–12129

690  
691 Brain CK. 1985. Temperature-induced changes in Africa as evolutionary stimuli. In *Species*  
692 *and Speciation*, ed. ES Vrba, pp. 45-52. Pretoria, Transvaal Museum Monograph  
693  
694 Brown FH, Sarna-Wojcicki AM, Meyer CE, Haileab B. 1992. Correlation of Pliocene and  
695 Pleistocene tephra layers between the Turkana Basin of East Africa and the Gulf of Aden.  
696 *Quat. Int.* 13:55–67  
697  
698 Brown FH, McDougall I, Fleagle JG. 2012. Correlation of the KHS Tuff of the Kibish  
699 Formation to volcanic ash layers at other sites, and the age of early *Homo sapiens* (Omo I and  
700 Omo II). *J. Hum. Evol.* 63:577–585  
701  
702 Brunet M, Guy F, Pilbeam D, Mackaye HT, Likius A, et al. 2002. A new hominid from the  
703 Upper Miocene of Chad, Central Africa. *Nature* 418:145–151  
704  
705 Burke K, Gunnell Y. 2008. The African Erosion Surface: a continental scale synthesis of  
706 geomorphology, tectonics, and environmental change over the past 180 million years. *Geol.*  
707 *Soc. Am. Mem.* 201:1–66  
708  
709 Caley T, Roche DM, Renssen H. 2014. Orbital Asian summer monsoon dynamics revealed  
710 using an isotope-enabled global climate model. *Nat. Commun.* 5:5371  
711  
712 Caley T, Extier T, Collins JA, Schefuß E, Dupont L, et al. 2018. A two-million-year-long  
713 hydroclimatic context for hominin evolution in southeastern Africa. *Nature* 560:76–79  
714  
715 Campisano C, Cohen AS, Arrowsmith JR, Asrat A, Behrensmeyer AK, et al. 2017. The  
716 Hominin Sites and Paleolakes Drilling Project: High-resolution paleoclimate records from the  
717 East African Rift System and their implications for understanding the environmental context  
718 of hominin evolution. *PaleoAnthropology* 2017:1–43  
719  
720 Cenozoic CO2 Proxy Integration Project (CenCO2PIP) Consortium et al. 2023. Toward a  
721 Cenozoic history of atmospheric CO2. *Science* 382:ead5177  
722  
723 Cerling TE. 2014. Stable isotope evidence for hominin environments in Africa. In *Treatise on*  
724 *Geochemistry*, Vol. 14: *Archaeology and Anthropology*, ed. TE Cerling, pp. 157–67. Oxford,  
725 UK: Pergamon. 2nd ed.  
726  
727 Chen M, Xie P, Janowiak JE, Arkin PA. 2002. Global Land Precipitation: A 50-yr Monthly  
728 Analysis Based on Gauge Observations. *J. Hydrometeorol.* 3:249–266  
729  
730 Cohen AS, Campisano CJ, Arrowsmith JR, Asrat A, Beck CC, et al. 2022. Reconstructing the  
731 environmental context of human origins in Eastern Africa through Scientific Drilling. *Annu.*  
732 *Rev. Earth Planet. Sci.* 50:451–476  
733  
734 Collins JA, Prange M, Caley T, Gimeno L, Beckmann B, et al. 2017. Rapid termination of the  
735 African Humid Period triggered by northern high-latitude cooling. *Nat. Commun.* 8:1372  
736  
737 Courtillot V, Davaille A, Besse J, Stock J. 2003. Three distinct types of hotspots in the  
738 Earth’s mantle. *Earth Planet. Sci. Lett.* 205:295–308  
739

740 Craig H, Gordon L. 1965. Deuterium and oxygen 18 variations in the ocean and the marine  
741 atmosphere. In *Stable Isotopes in Oceanographic Studies and Paleotemperatures*, ed. E  
742 Tongioli, pp. 9-130. Pisa: CNR Lab. Geol. Nucl.

743

744 Dart RA. 1925. *Australopithecus africanus*: the man-ape of South Africa. *Nature* 115:195–99

745 Darwin C. 1871. *The Descent of Man and Selection in Relation to Sex*. London: John Murray

746

747 d’Errico F, Banks WE, Warren DL, Sgubin G, van Niekerk K, et al. 2017. Identifying early  
748 modern human ecological niche expansions and associated cultural dynamics in the South  
749 African Middle Stone Age. *PNAS* 114:7869–7876

750

751 Delagnes A, Galland A, Gravina B, Bertran P, Corbé M, et al. 2023. Long-term behavioral  
752 adaptation of Oldowan toolmakers to resource-constrained environments at 2.3 Ma in the  
753 Lower Omo Valley (Ethiopia). *Sci. Rep.* 13:14350

754 Dirks PHGM, Berger LR. 2013. Hominin-bearing caves and landscape dynamics in the  
755 Cradle of Humankind, South Africa. *J. Afr. Earth Sci.* 78:109–31

756 Dupont LM, Donner B, Vidal L, Pérez EM, Wefer G. 2005. Linking desert evolution and  
757 coastal upwelling: Pliocene climate change in Namibia. *Geology* 33:461–464

758

759 Dupont LM, Rommerskirchen F, Mollenhauer G, Schefuß E. 2013. Miocene to Pliocene  
760 changes in South African hydrology and vegetation in relation to the expansion of C<sub>4</sub> plants.  
761 *Earth Planet. Sci. Lett.* 375:408–417

762 Dupont LM, Caley T, Castañeda IS. 2019. Effects of atmospheric CO<sub>2</sub> variability of the past  
763 800 kyr on the biomes of southeast Africa. *Clim. Past* 15:1083–1097

764

765 de Menocal PB. 1995. Plio-Pleistocene African climate. *Science* 270:53–59

766 de Menocal PB, Brown FH, Agustí J, Rook L, Andrews P. 1999. Pliocene tephra correlations  
767 between East African hominid localities, the Gulf of Aden, and the Arabian Sea. In *Hominid*  
768 *Evolution and Climatic Change in Europe*, ed. J Agustí, L Rook, P Andrews, pp. 23–54.  
769 Cambridge, UK: Cambridge Univ. Press

770 de Menocal PB. 2004. African climate change and faunal evolution during the Pliocene–  
771 Pleistocene. *Earth Planet. Sci. Lett.* 220:3–24

772

773 Elderfield H, Ferretti P, Greaves M, Crowhurst S, McCave IN, et al. 2012. Evolution of ocean  
774 temperature and ice volume through the mid-Pleistocene climate transition. *Science* 337:704–  
775 709

776

777 Eriksson A, Betti L, Friend AD, Lycett SJ, Singarayer JS, et al. 2012. Late Pleistocene  
778 climate change and the global expansion of anatomically modern humans. *PNAS* 109:16089–  
779 16094

780

781 Faith JT, Du A, Behrensmeier AK, Davies B, Patterson DB, et al. 2021. Rethinking the  
782 ecological drivers of hominin evolution. *Trends Ecol. Evol.* 36:797–807

783

784 Feakins SJ, Brown FH, de Menocal PB. 2007. Plio-Pleistocene microtephra in DSDP site 231,  
785 Gulf of Aden. *J. Afr. Earth Sci.* 48:341–352

786  
787 Feakins SJ, Levin NE, Liddy HM, Sieracki A, Eglinton TI, Bonnefille R. 2013. Northeast  
788 African vegetation change over 12 m.y. *Geology* 41:295–98  
789  
790 Gat JR. 1996. Oxygen and hydrogen isotopes in the hydrologic cycle. *Annu. Rev. Earth*  
791 *Planet. Sci.* 24:225–62  
792  
793 Geen R, Bordoni S, Battisti DS, Hui K. 2020. Monsoons, ITCZs, and the concept of the  
794 global monsoon. *Rev. Geophys.* 58:e2020RG000700  
795  
796 Gibert C, Vignoles A, Contoux C, Banks WE, Barboni D, et al. 2022. Climate-inferred  
797 distribution estimates of mid-to-late Pliocene hominins. *Glob. Planet. Change* 210:103756  
798  
799 Grant KM, Rohling EJ, Westerhold T, Zabel M, Heslop D. 2017. A 3 million year index for  
800 North African humidity/aridity and the implication of potential pan-African Humid periods.  
801 *Quat. Sci. Rev.* 171:100–118  
802  
803 Guan K, Wood EF, Medvigy D, Kimball J, Pan M, et al. 2014. Terrestrial hydrological  
804 controls on land surface phenology of African savannas and woodlands. *J. Geophys. Res.*  
805 *Biogeosci.* 119:1652–69  
806  
807 Hagen O. 2023. Coupling eco-evolutionary mechanisms with deep-time environmental  
808 dynamics to understand biodiversity patterns. *Ecography* 2023:e06132  
809  
810 Hakim G, Annan J, Brönnimann S, Crucifix M, Edwards T, et al. 2013. Overview of data  
811 assimilation methods. *PAGES news* 21  
812  
813 Hammer Ø, Harper DAT, Ryan PD. 2001. PAST: Paleontological statistics software package  
814 for education and data analysis. *Palaeont. Electr.* 4:9  
815  
816 Hartnady CJH, Partridge TC. 1995. Neotectonic uplift in southern Africa: a brief review and  
817 geodynamic conjecture. *Centennial Geocongress, Extended Abstracts* 456–459  
818  
819 Hempson GP, Archibald S, Bond WJ. 2015. A continent-wide assessment of the form and  
820 intensity of large mammal herbivory in Africa. *Science* 350:1056–1061  
821  
822 Hilgen FJ, Abels HA, Kuiper KF, Lourens LJ, Wolthers M. 2015. Towards a stable  
823 astronomical time scale for the Paleocene: Aligning Shatsky Rise with the Zumaia–Walvis  
824 Ridge ODP Site 1262 composite. *Newsl. Stratigr.* 48:91–110  
825  
826 Hilgen F, Zeeden C, Laskar J. 2020. Paleoclimate records reveal elusive~ 200-kyr eccentricity  
827 cycle for the first time. *Glob. Planet. Change* 194:103296  
828  
829 Hoetzel S, Dupont L, Schefuß E, Rommerskirchen F, Wefer G. 2013. The role of fire in  
830 Miocene to Pliocene C<sub>4</sub> grassland and ecosystem evolution. *Nat. Geosci.* 6:1027–30  
831  
832 Hoetzel S, Dupont LM, Wefer G. 2015. Miocene–Pliocene vegetation change in south-  
833 western Africa (ODP Site 1081, offshore Namibia). *Palaeogeogr. Palaeoclimatol.*  
834 *Palaeoecol.* 423:102–108

835 Hopley PJ, Maslin MA. 2010. Climate-averaging of terrestrial faunas: an example from the  
836 Plio-Pleistocene of South Africa. *Paleobiology*, 36:32–50  
837  
838 Howard E, Washington R. 2019. Drylines in southern Africa: Rediscovering the Congo air  
839 boundary. *J. Clim.* 32:8223–8242  
840  
841 Huang Y, Clemens SC, Liu W, Wang Y, Prell WL. 2007. Large-scale hydrological change  
842 drove the late Miocene C<sub>4</sub> plant expansion in the Himalayan foreland and Arabian Peninsula.  
843 *Geology* 35:531–534  
844  
845 Hutchison W, Fusillo R, Pyle DM, Mather TA, Blundy JD, et al. 2016. A pulse of mid-  
846 Pleistocene rift volcanism in Ethiopia at the dawn of modern humans. *Nat. Commun.* 7:13192  
847  
848 Joordens JC, Feibel CS, Vonhof HB, Schulp AS, Kroon D. 2019. Relevance of the eastern  
849 African coastal forest for early hominin biogeography. *J. Hum. Evol.* 131:176–202  
850  
851 Kaboth-Bahr S, Gosling WD, Vogelsang R, Bahr A, Scerri EM, et al. 2021. Paleo-ENSO  
852 influence on African environments and early modern humans. *PNAS* 118:e2018277118  
853  
854 Kashiwaya K, Ochiai S, Sakai H, Kawai T. 2001. Orbit-related long-term climate cycles  
855 revealed in a 12-Myr continental record from Lake Baikal. *Nature* 410:71–74  
856  
857 Kingston JD. 2007. Shifting adaptive landscapes: progress and challenges in reconstructing  
858 early hominid environments. *Yearb. Phys. Anthropol.* 50:20–58  
859  
860 Koutsodendris A, Nakajima K, Kaboth-Bahr S, Berke MA, Franzese AM, et al. 2021. A Plio-  
861 Pleistocene (c. 0–4 Ma) cyclostratigraphy for IODP Site U1478 (Mozambique Channel, SW  
862 Indian Ocean): Exploring an offshore record of paleoclimate and ecosystem variability in SE  
863 Africa. *Newsl. Stratigr.* 54:159–181  
864  
865 Kuechler RR, Schefuß E, Beckmann B, Dupont L, Wefer G. 2013. NW African hydrology  
866 and vegetation during the Last Glacial cycle reflected in plant-wax-specific hydrogen and  
867 carbon isotopes. *Quat. Sci. Rev.* 82:56–67  
868  
869 Kuechler RR, Dupont LM, Schefuß E. 2018. Hybrid insolation forcing of Pliocene monsoon  
870 dynamics in West Africa. *Clim. Past* 14:73–84  
871  
872 Laskar J, Robutel P, Joutel F, Gastineau M, Correia AC, Levrard B. 2004. A long-term  
873 numerical solution for the insolation quantities of the Earth. *A&A* 428:261–285  
874  
875 Lawrence KT, Liu Z, Herbert TD. 2006. Evolution of the eastern tropical Pacific through  
876 Plio-Pleistocene glaciation. *Science* 312:79–83  
877  
878 Leakey R, Leakey M. 1986. A new Miocene hominoid from Kenya. *Nature* 324:143–146  
879  
880 Lepre CJ, Quinn RL. 2022. Aridification and orbital forcing of eastern African climate during  
881 the Plio-Pleistocene. *Glob. Planet. Change* 208:103684  
882  
883 Levin NE. 2015. Environment and climate of early human evolution. *Annu. Rev. Earth*  
884 *Planet. Sci.* 43:405–429

885  
886 Liddy HM, Feakins SJ, Tierney JE. 2017. Cooling and drying in northeast Africa across the  
887 Pliocene. *Earth Planet. Sci. Lett.* 449:430–38  
888  
889 Lisiecki LE, Raymo ME. 2005. A Pliocene-Pleistocene stack of 57 globally distributed  
890 benthic  $\delta^{18}\text{O}$  records. *Paleoceanography* 20:PA1003  
891  
892 Lisiecki LE, Stern JV. 2016. Regional and global benthic  $\delta^{18}\text{O}$  stacks for the last glacial cycle.  
893 *Paleoceanography* 31:1368–1394  
894  
895 Lupien RL, Russell JM, Pearson EJ, Castañeda IS, Asrat A, et al. 2022. Orbital controls on  
896 eastern African hydroclimate in the Pleistocene. *Sci. Rep.* 12:3170  
897  
898 Lupien R, Uno K, Rose C, deRoberts N, Hazan C, et al. 2023. Low-frequency orbital  
899 variations controlled climatic and environmental cycles, amplitudes, and trends in northeast  
900 Africa during the Plio-Pleistocene. *Commun. Earth Environ.* 4:360  
901  
902 Macho GA. 2014. Baboon feeding ecology informs the dietary niche of *Paranthropus boisei*.  
903 *PLOS ONE* 9:e84942.  
904  
905 Macho GA. 2014b. An ecological and behavioural approach to hominin evolution during the  
906 Pliocene. *Quat. Sci. Rev.* 96:23–31  
907  
908 Macho GA. 2015. Pliocene hominin biogeography and ecology. *J. Hum. Evol.* 87:78–86  
909  
910 Maslin MA, Brierley CM, Milner AM, Shultz S, Trauth MH, Wilson KE. 2014. East African  
911 climate pulses and early human evolution. *Quat. Sci. Rev.* 101:1–17  
912  
913 Maxwell SJ, Hopley PJ, Upchurch P, Soligo C. 2018. Sporadic sampling, not climatic forcing,  
914 drives observed early hominin diversity. *PNAS* 115:4891–4896  
915  
916 McDougall I, Brown FH. 2009. Timing of volcanism and evolution of the northern Kenya  
917 Rift. *Geol. Mag.* 146:34–47  
918  
919 McNulty KP, Begun DR, Kelley J, Manthi FK, Mbua EN. 2015. A systematic revision of  
920 *Proconsul* with the description of a new genus of early Miocene hominoid. *J. Hum. Evol.*  
921 84:42–61  
922  
923 Mitsunaga BA, Lupien RL, Ouertani S, Stubbs B, Deino AL, et al. 2023. High-latitude, Indian  
924 Ocean, and orbital Influences on eastern African hydroclimate across the Plio-Pleistocene  
925 boundary. *Paleoceanogr. Paleoclimatol.* 38:e2023PA004671  
926  
927 Mohtadi M, Prange M, Steinke S. 2016. Palaeoclimatic insights into forcing and response of  
928 monsoon rainfall. *Nature* 533:191–199  
929  
930 Moore A, Blenkinsop TG, Cotterill F, 2009. Southern African topography and erosion  
931 history: plumes or plate tectonics? *Terra Nova* 21:310–315  
932  
933 Morley R, Richards K. 1993. Gramineae cuticle: a key indicator of Late Cenozoic climatic  
934 change in the Niger Delta. *Rev. Palaeobot. Palynol.* 77:119–127

935  
936 Munday C, Savage N, Jones RG, Washington R. 2023. Valley formation aridifies East Africa  
937 and elevates Congo Basin rainfall. *Nature* 615:276–279  
938  
939 Nengo I, Tafforeau P, Gilbert CC, Fleagle JG, Miller ER, et al. 2017. New infant cranium  
940 from the African Miocene sheds light on ape evolution. *Nature* 548:169–174  
941  
942 Nicholson SE, Sharon E. 2013. The West African Sahel: A review of recent studies on the  
943 rainfall regime and its interannual variability. *Int. Sch. Res. Notices* 2013  
944  
945 Niespolo EM, WoldeGabriel G, Hart WK, Renne PR, Sharp WD, et al. 2021. Integrative  
946 geochronology calibrates the Middle and Late Stone Ages of Ethiopia’s Afar Rift. *PNAS*  
947 118:e2116329118  
948  
949 O'Brien K, Hebdon N, Faith JT. 2023. Paleoecological evidence for environmental  
950 specialization in *Paranthropus boisei* compared to early *Homo*. *J. Hum. Evol.* 177:103325  
951  
952 O’Mara NA, Skonieczny C, McGee D, Winckler G, Bory AJM, et al. 2022. Pleistocene  
953 drivers of Northwest African hydroclimate and vegetation. *Nat. Commun.* 13:3552  
954  
955 Partridge TC. 1998. Of diamonds, dinosaurs and diastrophism: 150 million years of landscape  
956 evolution in southern Africa. *S. Afr. J. Geol.* 101:167–184  
957  
958 Patterson DB, Du A, Faith JT, Rowan J, Uno K, et al. 2022. Did vegetation change drive the  
959 extinction of *Paranthropus boisei*? *J. Hum. Evol.* 173:103154  
960  
961 Peppe DJ, Cote SM, Deino AL, Fox DL, Kingston JD, et al. 2023. Oldest evidence of  
962 abundant C<sub>4</sub> grasses and habitat heterogeneity in eastern Africa. *Science* 380:173–177  
963  
964 Pires MM, Silvestro D, Quental TB. 2017. Interactions within and between clades shaped the  
965 diversification of terrestrial carnivores. *Evolution* 71:1855–1864  
966  
967 Plummer TW, Ditchfield PW, Bishop LC, Kingston JD, Ferraro JV, et al. 2009. Oldest  
968 evidence of toolmaking hominins in a grassland-dominated ecosystem. *PLOS ONE* 4:e7199  
969  
970 Plummer TW, Oliver JS, Finestone EM, Ditchfield PW, Bishop LC, et al. 2023. Expanded  
971 geographic distribution and dietary strategies of the earliest Oldowan hominins and  
972 *Paranthropus*. *Science* 379:561–566  
973  
974 Polissar PJ, Rose C, Uno K, Phelps SR, de Menocal P. 2019. Synchronous rise of African C<sub>4</sub>  
975 ecosystems 10 million years ago in the absence of aridification. *Nat. Geosci.* 12:657–60  
976  
977 Potts R. 1995. Environmental variability and its effect on hominid evolution. *Acta*  
978 *Anthropologica Sinica* 14:324  
979  
980 Potts R. 1996. Evolution and climate variability. *Science* 273:922–23  
981  
982 Potts R. 1998. Variability selection in hominid evolution. *Evol. Anthropol.* 7:81–96  
983

984 Potts R. 2013. Hominin evolution in settings of strong environmental variability. *Quat. Sci.*  
985 *Rev.* 73:1–13  
986  
987 Potts R, Behrensmeyer AK, Faith JT, Tryon CA, Brooks AS, et al. 2018. Environmental  
988 dynamics during the onset of the Middle Stone Age in eastern Africa. *Science* 360:86–90  
989  
990 Potts R, Dommain R, Moerman JW, Behrensmeyer AK, Deino AL, et al. 2020. Increased  
991 ecological resource variability during a critical transition in hominin evolution. *Sci. Adv.*  
992 6:eabc8975  
993  
994 Price SA, Hopkins SS, Smith KK, Roth VL. 2012. Tempo of trophic evolution and its impact  
995 on mammalian diversification. *PNAS* 109:7008–7012  
996  
997 Reed KE. 1997. Early hominid evolution and ecological change through the African Plio-  
998 Pleistocene. *J. Hum. Evol.* 32:289–322  
  
999 Roberts HM, Ramsey CB, Chapot MS, Deino AL, Lane CS, et al. 2021. Using multiple  
1000 chronometers to establish a long, directly-dated lacustrine record: constraining >600,000  
1001 years of environmental change at Chew Bahir, Ethiopia. *Quat. Sci. Rev.* 266:107025  
1002  
1003 Roberts EM, Stevens NJ, O’Connor PM, Dirks PHGM, Gottfried MD, et al. 2012. Initiation  
1004 of the western branch of the East African Rift coeval with the eastern branch. *Nat. Geosci.*  
1005 5:289–94  
1006  
1007 Robinson JR, Rowan J, Campisano CJ, Wynn JG, Reed KE. 2017. Late Pliocene  
1008 environmental change during the transition from *Australopithecus* to *Homo*. *Nat. Ecol. Evol.*  
1009 1:0159  
1010  
1011 Rochette P, Tamrat E, Féraud G, Pik R, Courtillot V, et al. 1998. Magnetostratigraphy and  
1012 timing of the Oligocene Ethiopian traps. *Earth Planet. Sci. Lett.* 164:497–510  
1013  
1014 Rohling EJ, Foster GL, Grant KM, Marino G, Roberts AP, et al. 2014. Sea-level and deep-  
1015 sea-temperature variability over the past 5.3 million years. *Nature* 508:477–482  
1016  
1017 Rohling EJ, Yu J, Heslop D, Foster GL, Opdyke B, Roberts AP. 2021. Sea level and deep-sea  
1018 temperature reconstructions suggest quasi-stable states and critical transitions over the past 40  
1019 million years. *Sci. Adv.* 7:eabf5326.  
1020  
1021 Rose C, Polissar PJ, Tierney JE, Filley T, de Menocal PB. 2016. Changes in northeast African  
1022 hydrology and vegetation associated with Pliocene–Pleistocene sapropel cycles. *Philos.*  
1023 *Trans. R. Soc. Lond. B Biol. Sci.* 371:20150243  
1024  
1025 Rowan J, Kamilar JM, Beaudrot L, Reed KE. 2016. Strong influence of palaeoclimate on the  
1026 structure of modern African mammal communities. *Proc. R. Soc. B: Biol. Sci.* 283:20161207  
1027  
1028 Ruan J, Timmermann A, Raia P, Yun KS, Zeller E, et al. 2023. Climate shifts orchestrated  
1029 hominin interbreeding events across Eurasia. *Science* 381:699–704  
1030  
1031 Rubbelke CB, Bhattacharya T, Feng R, Burls NJ, Knapp S, McClymont EL. 2023. Plio-  
1032 Pleistocene southwest African hydroclimate modulated by Benguela and Indian Ocean  
1033 temperatures. *Geophys. Res. Lett.* 50:e2023GL103003



1034  
1035 Sachse D, Billault I, Bowen GJ, Chikaraishi Y, Dawson TE, et al. 2012. Molecular  
1036 paleohydrology: interpreting the hydrogen-isotopic composition of lipid biomarkers from  
1037 photosynthesizing organisms. *Annu. Rev. Earth Planet. Sci.* 40:221–249  
1038  
1039 Sahle Y, Hutchings WK, Braun DR, Sealy JC, Morgan LE, et al. 2013. Earliest stone-tipped  
1040 projectiles from the Ethiopian Rift date to >279,000 years ago. *PLOS ONE* 8:e78092  
1041  
1042 Sahle Y, Beyene Y, Defleur A, Asfaw B, WoldeGabriel G, Hart WK. 2019. Human  
1043 emergence: Perspectives from Herto, Afar Rift, Ethiopia. In *Modern human origins and*  
1044 *dispersal*, ed. Y Sahle, H Reyes Centeno, C Bentz, pp; 105-136. Tübingen, Kerns Verlag  
1045  
1046 Sarna-Wojcicki AM, Meyer CE, Roth PH, Brown FH. 1985. Ages of tuff beds at East African  
1047 early hominid sites and sediments in the Gulf of Aden. *Nature* 313:306–308  
1048  
1049 Scerri EM, Chikhi L, Thomas MG. 2019. Beyond multiregional and simple out-of-Africa  
1050 models of human evolution. *Nat. Ecol. Evol.* 3:1370–1372  
1051  
1052 Schefuß E, Schouten S, Schneider RR. 2005. Climatic controls on central African hydrology  
1053 during the past 20,000 years. *Nature* 437:1003–6  
1054  
1055 Schefuß E, Dupont LM. 2020. Multiple drivers of Miocene C<sub>4</sub> ecosystem expansions. *Nat.*  
1056 *Geosci.* 13:463–464  
1057  
1058 Schneider T, Bischoff T, Haug GH. 2014. Migrations and dynamics of the intertropical  
1059 convergence zone. *Nature* 513:45–53.  
1060  
1061 Schulz M, Mudelsee M. 2002. REDFIT: estimating red-noise spectra directly from unevenly  
1062 spaced paleoclimatic time series. *Comput. Geosci.* 28:421–426  
1063  
1064 Sepulchre P, Ramstein G, Fluteau F, Schuster M, Tiercelin JJ, Brunet M. 2006. Tectonic  
1065 uplift and eastern Africa aridification. *Science* 311:1419–23  
1066  
1067 Shackleton NJ. 1974. *Attainment of isotopic equilibrium between ocean water and benthonic*  
1068 *foraminifera genus Uvigerina: isotopic changes in the ocean during the last glacial*. Paper  
1069 presented at Colloque international du CNRS 219, Gif-sur-Yvette  
1070  
1071 Sithaldeen R, Ackermann RR, Bishop JM. 2015. Pleistocene aridification cycles shaped the  
1072 contemporary genetic architecture of Southern African baboons. *PLOS ONE* 10:e0123207  
1073  
1074 Skonieczny C, McGee D, Winckler G, Bory A, Bradtmiller LI, et al. 2019. Monsoon-driven  
1075 Saharan dust variability over the past 240,000 years. *Sci. Adv.* 5:eaav1887  
1076  
1077 Soberón J, Nakamura M. 2009. Niches and distributional areas: concepts, methods, and  
1078 assumptions. *PNAS* 106:19644–19650  
1079  
1080 Sørensen EF, Harris RA, Zhang L, Raveendran M, Kuderna LF, et al. 2023. Genome-wide  
1081 coancestry reveals details of ancient and recent male-driven reticulation in baboons. *Science*  
1082 380:eabn8153  
1083

1084 Sosdian S, Rosenthal Y. 2009. Deep-sea temperature and ice volume changes across the  
1085 Pliocene-Pleistocene climate transitions. *Science* 325:306–310  
1086  
1087 Souron A. 2018. Morphology, diet, and stable carbon isotopes: on the diet of *Theropithecus*  
1088 and some limits of uniformitarianism in paleoecology. *Am. J. Phys. Anthropol.* 166:261–267  
1089  
1090 Sponheimer M, Alemseged Z, Cerling TE, Grine FE, Kimbel WH, et al. 2013. Isotopic  
1091 evidence of early hominin diets. *PNAS* 110:10513-10518  
  
1092 Sternberg LDL. 1988. D/H ratios of environmental water recorded by D/H ratios of plant  
1093 lipids. *Nature* 333:59–61  
1094  
1095 Sturm C, Zhang Q, Noone D. 2010. An introduction to stable water isotopes in climate  
1096 models: benefits of forward proxy modelling for paleoclimatology. *Clim. Past* 6:115–129  
  
1097 Taylor AK, Berke MA, Castañeda IS, Koutsodendris A, Campos H, et al. 2021. Plio-  
1098 Pleistocene continental hydroclimate and Indian ocean sea surface temperatures at the  
1099 southeast African margin. *Paleoceanogr. Paleoclimatol.* 36:e2020PA004186  
1100  
1101 Tiedemann R, Sarnthein M, Shackleton NJ. 1994. Astronomic timescale for the Pliocene  
1102 Atlantic  $\delta^{18}\text{O}$  and dust flux records of Ocean Drilling Program Site 659. *Paleoceanography*  
1103 9:619-638  
1104  
1105 Tierney JE, Russell JM, Damsté JSS, Huang Y, Verschuren D. 2011. Late Quaternary  
1106 behavior of the East African monsoon and the importance of the Congo Air Boundary. *Quat.*  
1107 *Sci. Rev.* 30:798–807  
1108  
1109 Tierney JE, de Menocal PB, Zander PD. 2017. A climatic context for the out-of-Africa  
1110 migration. *Geology*, 45:1023–1026  
1111  
1112 Tierney JE, Zhu J, King J, Malevich SB, Hakim GJ, Poulsen, CJ. 2020a. Glacial cooling and  
1113 climate sensitivity revisited. *Nature* 584:569–573  
1114  
1115 Tierney JE, Poulsen CJ, Montañez IP, Bhattacharya T, Feng R, et al. 2020b. Past climates  
1116 inform our future. *Science* 370:eaay3701  
1117  
1118 Timmermann A, Friedrich T. 2016. Late Pleistocene climate drivers of early human  
1119 migration. *Nature* 538:92–95  
1120  
1121 Timmermann A, Yun KS, Raia P, Ruan J, Mondanaro A, et al. 2022. Climate effects on  
1122 archaic human habitats and species successions. *Nature* 604:495–501  
1123  
1124 Torrence C, Compo GP. 1998. A practical guide to wavelet analysis. *Bull. Am. Meteorol. Soc.*  
1125 79:61–78.  
1126  
1127 Trauth MH, Asrat A, Berner N, Bibi F, Foerster V, et al. 2021. Northern Hemisphere  
1128 Glaciation, African climate and human evolution. *Quat. Sci. Rev.* 268:107095  
1129  
1130 Uno KT, Polissar PJ, Jackson KE, de Menocal PB. 2016a. Neogene biomarker record of  
1131 vegetation change in eastern Africa. *PNAS* 113:6355–63  
1132

- 1133 Uno KT, Polissar PJ, Kahle E, Feibel C, Harmand S, et al. 2016b. A Pleistocene  
 1134 palaeovegetation record from plant wax biomarkers from the Nachukui Formation, West  
 1135 Turkana, Kenya. *PNAS* 371:20150235  
 1136
- 1137 Urey HC. 1947. Thermodynamic properties of isotopic substances. *J. Chem. Soc.* 562–581  
 1138
- 1139 Van der Lubbe HJL, Hall IR, Barker S, Hemming SR, Baars TF, et al. 2021. Indo-Pacific  
 1140 Walker circulation drove Pleistocene African aridification. *Nature* 598:618–623
- 1141 van Holstein LA, Foley RA. 2022. A process-based approach to hominin taxonomy provides  
 1142 new perspectives on hominin speciation. *Evol. Anthropol.*, 31:166–174
- 1143 Vermote E, Justice C, Csiszar I, Eidenshink J, Myneni R, et al. 2014. NOAA Climate Data  
 1144 Record (CDR) of Normalized Difference Vegetation Index (NDVI), Version 4. *NOAA*  
 1145 *National Centers for Environmental Information.*
- 1146 Vidal CM, Lane CS, Asrat A, Barfod DN, Mark DF, et al. 2022. Age of the oldest known  
 1147 *Homo sapiens* from eastern Africa. *Nature* 601:579–583  
 1148
- 1149 Vrba ES. 1985. Ecological and adaptive changes associated with early hominid evolution. In  
 1150 *Ancestors: The Hard Evidence*, ed. E Delson, pp. 63–71. New York: Liss
- 1151 Vrba ES. 1995. The fossil record of African antelopes (Mammalia, Bovidae) in relation to  
 1152 human evolution and paleoclimate. In *Paleoclimate and Evolution with Emphasis on Human*  
 1153 *Origins*, ed. ES Vrba, GH Denton, TC Partridge, LH Burckle, pp. 285–294. New Haven, CT:  
 1154 Yale Univ. Press
- 1155 Wara MW, Ravelo AC, Delaney ML. 2005. Permanent El Niño-like conditions during the  
 1156 Pliocene warm period. *Science* 309:758–761  
 1157
- 1158 Werdelin L, Lewis ME. 2005. Plio-Pleistocene Carnivora of eastern Africa: species richness  
 1159 and turnover patterns. *Zool. J. Linn. Soc.* 144:121–144  
 1160
- 1161 White F. 1983. *The vegetation of Africa—a descriptive memoir to accompany the*  
 1162 *UNESCO/AETFAT/UNSO vegetation map of Africa*. Nat. Resour. Res. Rep. XX, U.N. Educ.  
 1163 Sci. Cult. Org. (UNESCO), Paris
- 1164 White TD, Asfaw B, DeGusta D, Gilbert H, Richards GD, et al. 2003. Pleistocene *Homo*  
 1165 *sapiens* from Middle Awash, Ethiopia. *Nature* 423:742–747
- 1166 Woldegabriel G, Aronson JL, Walter RC. 1990. Geology, geochronology, and rift basin  
 1167 development in the central sector of the Main Ethiopia Rift. *Geol. Soc. Am. Bull.* 102 439–458  
 1168
- 1169 WoldeGabriel G, Walter RC, Aronson JL, Hart WK. 1992. Geochronology and distribution of  
 1170 silicic volcanic rocks of Plio-Pleistocene age from the central sector of the Main Ethiopian  
 1171 Rift. *Quat. Int.* 13:69–76  
 1172
- 1173 Wood B, Strait D. 2004. Patterns of resource use in early *Homo* and *Paranthropus*. *J. Hum.*  
 1174 *Evol.* 46:119–162  
 1175
- 1176 Wood B, Boyle EK. 2016. Hominin taxic diversity: Fact or fantasy? *Am. J. Phys. Anthropol.*  
 1177 159 37–78

1178  
1179 Wright S. 1932. The roles of mutation, inbreeding, crossbreeding and selection in evolution.  
1180 In *Proc Sixth Int Congress Genet*, pp. 356–366.  
1181  
1182 Wright S. 1968. *Evolution and the Genetics of Populations*. University of Chicago Press 1–4  
1183  
1184 Yun KS, Timmermann A, Lee SS, Willeit M, Ganopolski A, Jadhav J. 2023. A transient  
1185 coupled general circulation model (CGCM) simulation of the past 3 million years. *Clim. Past*  
1186 19:1951–1974  
1187  
1188 Zabel M, Bickert T, Dittert L, Haese RR. 1999. Significance of the sedimentary Al:Ti ratio as  
1189 an indicator for variations in the circulation patterns of the equatorial North Atlantic.  
1190 *Paleoceanography* 14:789–799  
1191  
1192 Zeller E, Timmermann A, Yun KS, Raia P, Stein K, Ruan J. 2023. Human adaptation to  
1193 diverse biomes over the past 3 million years. *Science* 380:604–608  
1194  
1195  
1196  
1197  
1198  
1199  
1200  
1201  
1202  
1203  
1204  
1205  
1206  
1207  
1208  
1209  
1210  
1211  
1212  
1213  
1214

1215 **OPTIONAL ELEMENTS**

1216 Reference Annotations:

1217 Vrba (1995): the turnover-pulse hypothesis: pulses of speciation/extinctions, and dispersals  
1218 across clades due to prolonged climatic changes.

1219 de Menocal (1995): Pioneering work based on marine cores that linked human evolution to  
1220 global climate change.

1221 Potts (1998): variability selection hypothesis: increased climatic variability as a driver for  
1222 genetic change (human's unique adaptability).

1223 Cerling (2014): summary of the use of stable isotopes to reconstruct hominin environments.

1224 Uno et al. (2016a): first Neogene biomarker records in marine cores.

1225 Faith et al. (2021): sampling biases affect our interpretation of the hominin fossil record, i.e.,  
1226 gaps in spatiotemporal sampling.

1227 Timmermann et al. (2022): first long transient climate simulation to identify the  
1228 spatiotemporal habitat suitability of hominin species.

1229 Ao et al. (2024): an example of data-model integrative approach that identify potential  
1230 dispersal corridors from Africa to Asia.

1231

1232

1233

1234

1235

1236

1237

1238

1239

1240

1241

1242

1243

1244

1245

1246

<b>Proxies</b>	<b>Climate/environmental variables</b>	<b>Potential biases/complexity</b>
δD plant waxes	Hydrological cycle (precipitation amount, circulation regime)	Source effect, seasonality, temperature effect, relative humidity, vegetation changes
δ <sup>13</sup> C plant waxes	Vegetation (biomass, C <sub>3</sub> vs C <sub>4</sub> plants)	Source effect, plant physiological versus climatic parameters, seasonal timing of leaf wax formation, effect of vegetation
Pollen	Vegetation	Actualism, Plant physiological versus climatic parameters, seasonal timing of pollen formation, transport effect and mode of transport (river vs wind)
XRF ratio	Wet-dry index; wet: high terrestrial input via river; dry: low terrestrial input via river	Source in the catchment and vegetation role on sediment load, sea level effect
Terrestrial organic carbon (C <sub>org</sub> ; BIT)	Wet: increased terrigenous organic matter supply by river; dry: decreased terrigenous organic matter supply by river	Diagenesis, source in the catchment
Dust	Wet: less dust input into the Ocean; dry: more dust input into the Ocean	Source effect, wind strength and transport effect, calculation of fluxes
Radiogenic isotope signatures of detrital material (ε <sub>nd</sub> )	Provenance, dispersal, and climate-driven supply of sediments	Source. Grain size effects.
Ba/Ca and δ <sup>18</sup> O <sub>sea water</sub> in planktonic foraminifera	Riverine freshwater input	Source effect, changes in atmospheric circulation, advection, sea level effect

1247 Table 1: Main proxies for terrestrial climate and environmental reconstructions in marine  
1248 sediment cores.

1249

1250

1251

1252

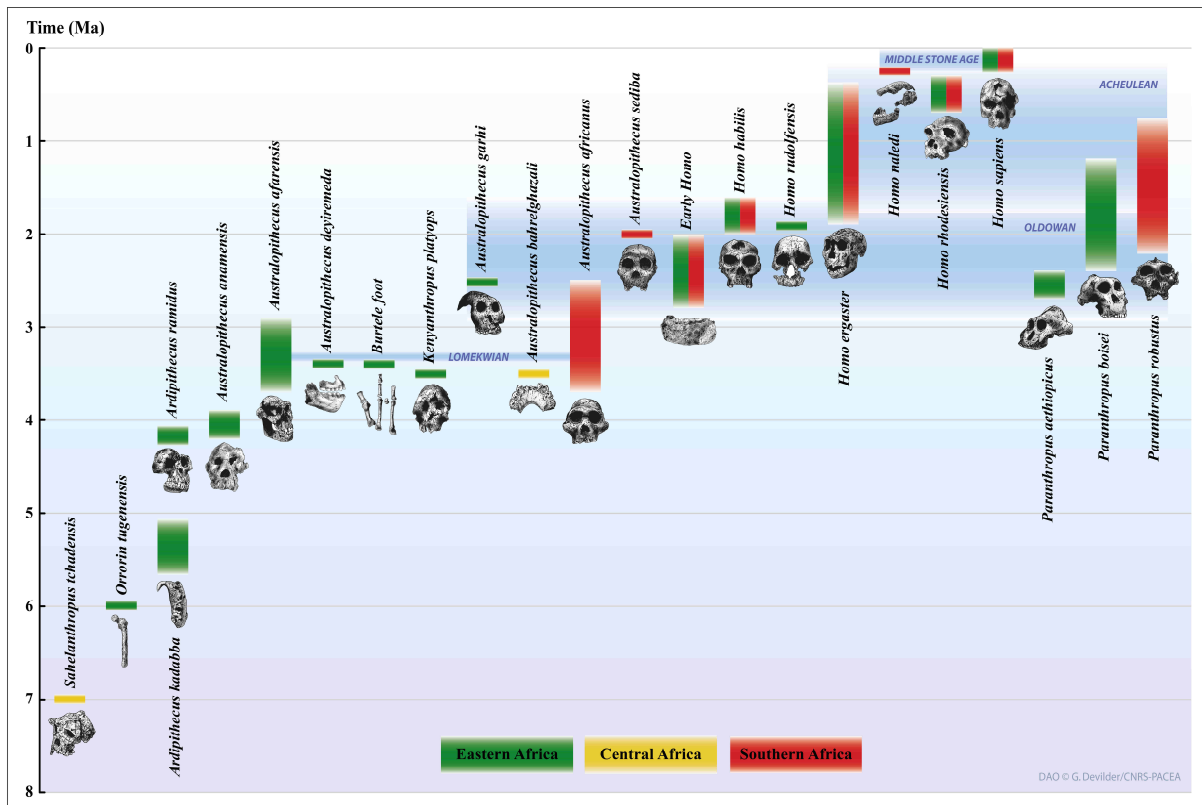
1253

1254

1255

1256

1257



1259

1260

1261 Figure 1: Stratigraphic ranges of African hominin taxa and associated lithic industries.  
 1262 Modified after Sahle et al. (2013), Beyene et al. (2013), Wood & Boyle (2016), Plummer et  
 1263 al. (2023) and references herein. Hominin taxonomy is debated and actual paleobiodiversity  
 1264 may be partly overestimated by taxinomic practices or underestimated due to taphonomic  
 1265 issues, making it extremely difficult to have a clear understanding of the real  
 1266 paleobiodiversity.

1267

1268

1269

1270

1271

1272

1273

1274

1275

1276

1277

1278  
1279  
1280  
1281  
1282  
1283  
1284  
1285  
1286  
1287  
1288  
1289  
1290  
1291  
1292  
1293  
1294  
1295  
1296  
1297  
1298  
1299  
1300  
1301  
1302  
1303  
1304  
1305  
1306  
1307  
1308

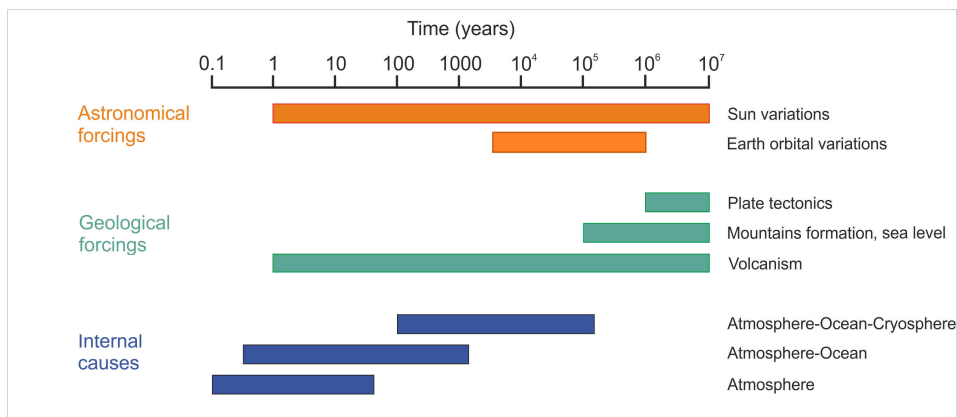


Figure 2: Schematic of main natural forcings/causes of climate changes (adapted from Bard 2002).



1309  
1310  
1311  
1312  
1313  
1314  
1315  
1316  
1317  
1318  
1319  
1320  
1321  
1322  
1323  
1324  
1325  
1326  
1327  
1328  
1329  
1330  
1331  
1332  
1333  
1334  
1335  
1336  
1337  
1338  
1339  
1340

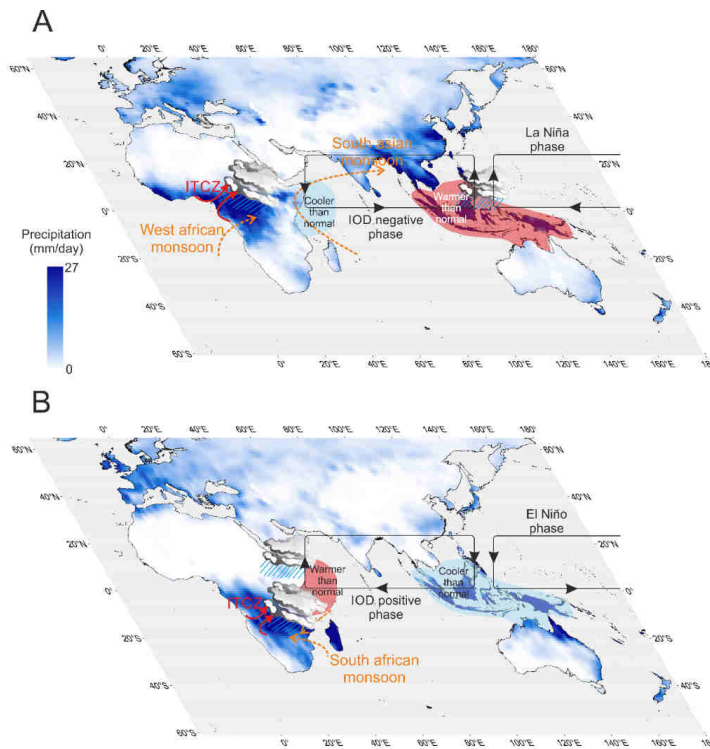


Figure 3: Main modern hydroclimate processes and changes at low latitudes and their impact on Africa. A. Averaged precipitation rates for August and B. January (Chen et al. 2002). Tropical inter-annual climate variabilities (ENSO: El Niño Southern Oscillation and IOD: Indian Ocean Dipole) are illustrated as examples of configuration but not necessary entirely dependent and are not necessarily linked with latitudinal variability (ITCZ: InterTropical Convergence Zone migration, size and strength and regional monsoon systems).

1341  
1342  
1343  
1344  
1345  
1346  
1347  
1348  
1349  
1350  
1351  
1352  
1353  
1354  
1355  
1356  
1357  
1358  
1359  
1360  
1361  
1362  
1363  
1364  
1365  
1366  
1367  
1368  
1369  
1370  
1371

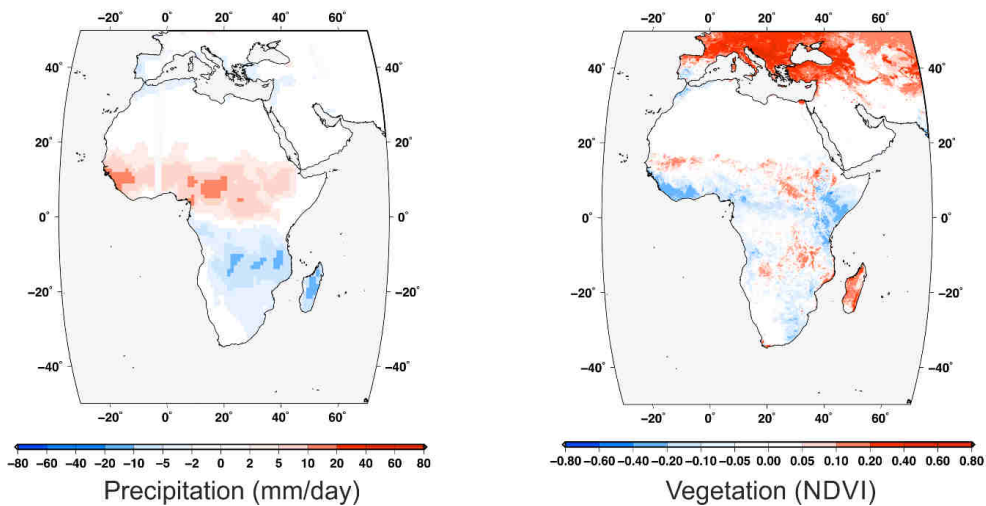


Figure 4: Anomaly (August-January) for precipitation (Chen et al. 2002) and vegetation (NDVI: Normalized Difference Vegetation Index) in Africa (Vermote et al. 2014). NDVI quantifies vegetation by measuring the difference between near-infrared (which vegetation strongly reflects) and red light (which vegetation absorbs).

1372  
1373  
1374  
1375  
1376  
1377  
1378  
1379  
1380  
1381  
1382  
1383  
1384  
1385  
1386  
1387  
1388  
1389  
1390  
1391  
1392  
1393  
1394  
1395  
1396  
1397  
1398  
1399  
1400  
1401  
1402  
1403

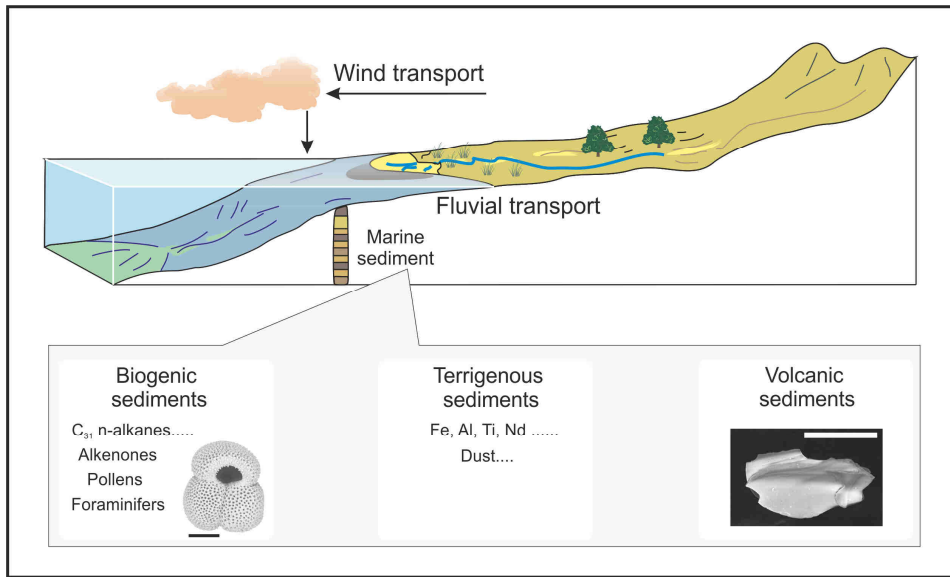
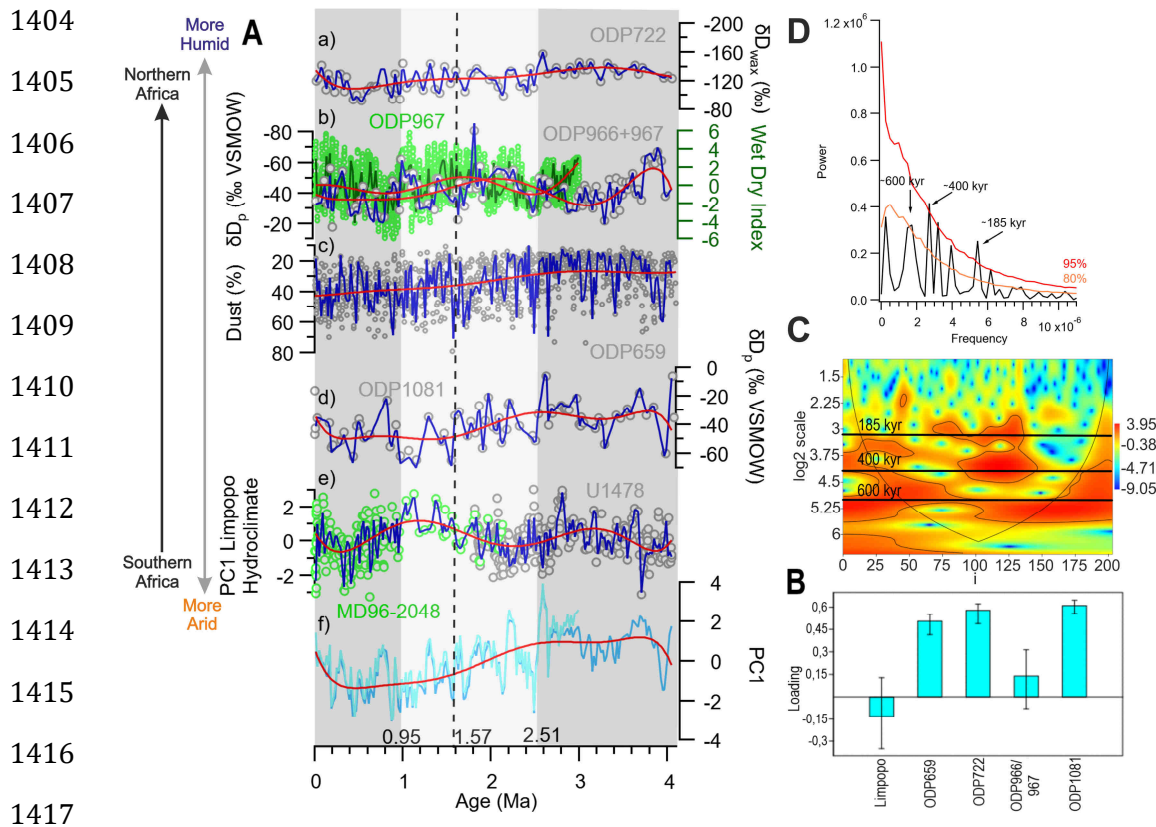


Figure 5: Scheme of sediment transport from the continent (source) to the ocean (sink) and main sediments in marine environment. SEM images from marine sediments (left to right) of the planktonic foraminifera *G. ruber*, and volcanic glass shard from the East African Rift System (indicated scale is 100 $\mu$ m).



1418 Figure 6: Pan-African hydroclimate variability over the last 4 Myr based on marine sediment  
 1419 cores. A. a)  $\delta D$  of the n- $C_{31}$  alkane of plant waxes at site ODP722 (Huang et al. 2007). b) Blue  
 1420 line shows  $\delta D$  of precipitation ( $\delta D_p$ ) at ODP966& 967 (Lupien et al. 2023). Standard error  
 1421 means was 4.3 ‰ for  $\delta D_p$ . Green line shows the Wet-Dry index from ODP967 (Grant et al.  
 1422 2017). c) Dust percentage at ODP659 (Tiedemann 1994). d)  $\delta D$  of precipitation derived from  
 1423 the vegetation correction of  $\delta D_{wax}$  at site ODP1081 (Rubbelke et al. 2023). The average  
 1424 standard deviation was 1.81 ‰ for  $\delta D_{wax}$  and mean error for  $\delta D$  of precipitation was 3.7 ‰. e)  
 1425 PC1 of hydroclimate records from the Limpopo region, sites MD96-2048 and IODP U1478  
 1426 (Caley et al. 2018, Koutsodendris et al. 2021, Taylor et al. 2021). f) PC1 of pan-African  
 1427 hydroclimate. Polynomial fit (8th degree) documented in red to demonstrate long-term trends  
 1428 and fluctuations. Grey shading and dash line depict the four phases that have been constrained  
 1429 by change point analysis based on records in a) to e). B. Average PC1 loadings derived from  
 1430 the PCA with bootstrapped confidence intervals (Past software, Hammer et al. 2001). C.  
 1431 Wavelet transform on the PC1 based on Torrence & Compo (1998). The significance level  
 1432 corresponding to  $p = 0.05$  is plotted as a contour (chi-squared test). D. Spectral analyses on  
 1433 the PC1 with REDFIT (Schulz & Mudelsee 2002, the red and orange lines show the false-  
 1434 alarm level at the 95 % and 80 % confidence interval).

1435  
 1436  
 1437  
 1438  
 1439

1440  
 1441  
 1442  
 1443  
 1444  
 1445  
 1446  
 1447  
 1448  
 1449  
 1450  
 1451  
 1452  
 1453  
 1454  
 1455  
 1456  
 1457  
 1458  
 1459  
 1460  
 1461  
 1462  
 1463  
 1464  
 1465  
 1466  
 1467  
 1468  
 1469  
 1470  
 1471  
 1472  
 1473  
 1474  
 1475  
 1476  
 1477  
 1478  
 1479  
 1480  
 1481  
 1482  
 1483  
 1484  
 1485  
 1486  
 1487

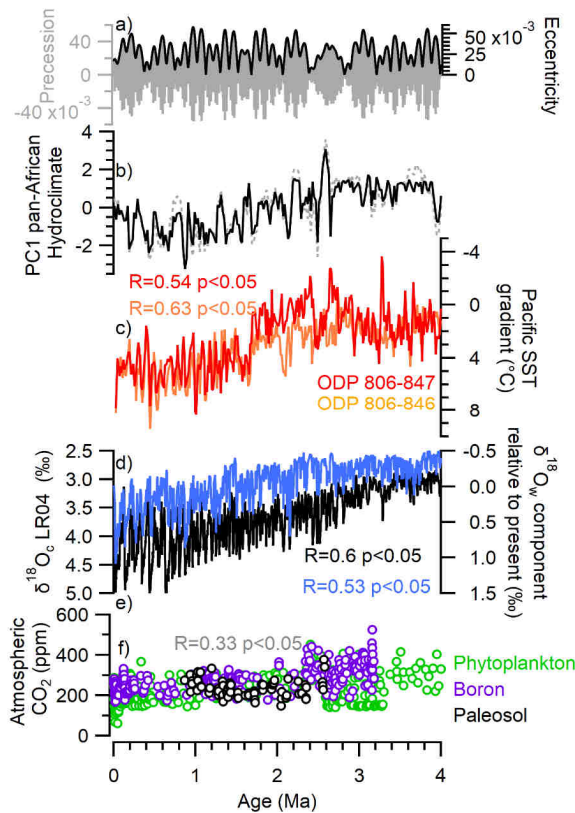


Figure 7: Forcings on pan-African hydroclimate. a) Eccentricity variations that modulate precession (Laskar et al. 2004). b) PC1 of pan-African hydroclimate original (dash line) and residue (solid line) after removal of orbital forcings variance. c) Pacific sea surface temperature (SST) gradients (sites ODP 806 and 847 (Wara et al. 2005), site ODP 846 (Lawrence et al. 2006)). d) Component of sea-level-based ocean  $\delta^{18}\text{O}_w$  variations (Rohling et al. 2014). e) Deep-sea  $\delta^{18}\text{O}_c$  LR04 stack (Lisiecki & Raymo 2005) (**see Appendices Water and Carbon isotopes**). f) Atmospheric  $\text{CO}_2$  reconstructions (The CenCO2PIP Consortium 2023). The correlation coefficient (R) and corresponding significance (P) between residual PC1 pan-African hydroclimate and SST gradients (c), ice volume changes (d and e) and atmospheric  $\text{CO}_2$  changes (f) are shown.

1488  
 1489  
 1490  
 1491  
 1492  
 1493  
 1494  
 1495  
 1496  
 1497  
 1498  
 1499  
 1500  
 1501  
 1502  
 1503  
 1504  
 1505  
 1506  
 1507  
 1508  
 1509  
 1510  
 1511  
 1512  
 1513  
 1514  
 1515  
 1516  
 1517  
 1518  
 1519

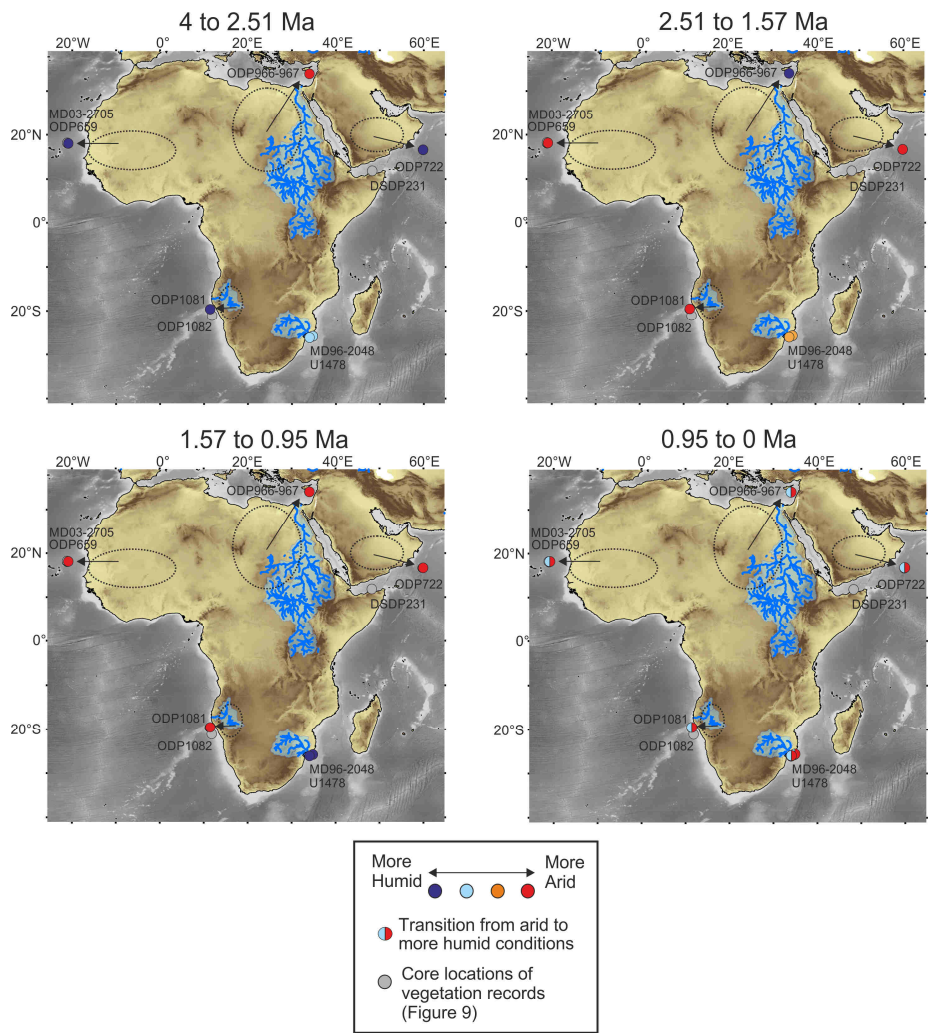


Figure 8: Major phases of pan-African hydroclimate variability. Main fluvial catchments that transport material to marine sediment cores are indicated together with the main source of material transported by winds to marine sites (see also Figure 11). Core locations with red/blue colors indicate more arid/humid hydroclimate. Core locations of vegetation records of Figure 9 are also indicated.

1520  
 1521  
 1522  
 1523  
 1524  
 1525  
 1526  
 1527  
 1528  
 1529  
 1530  
 1531  
 1532  
 1533  
 1534  
 1535  
 1536  
 1537  
 1538  
 1539  
 1540  
 1541  
 1542  
 1543  
 1544  
 1545  
 1546  
 1547  
 1548  
 1549  
 1550  
 1551  
 1552  
 1553  
 1554  
 1555  
 1556

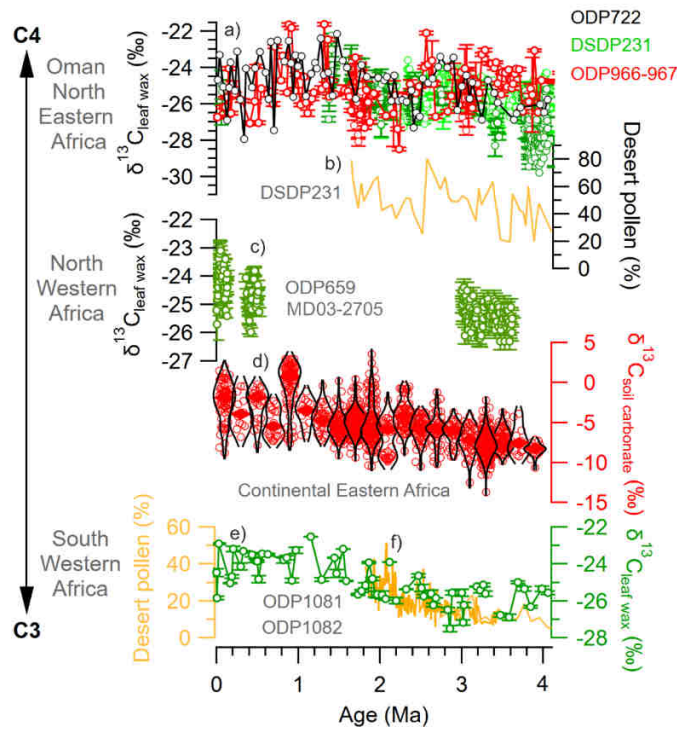
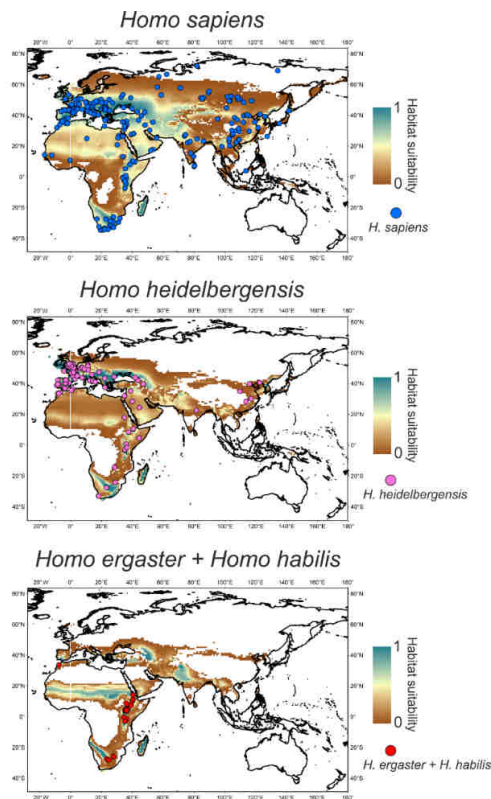


Figure 9: Pan-African vegetation variability over the last 4 Myr based mainly on ocean cores. a)  $\delta^{13}\text{C}_{\text{leaf wax}}$  from sites ODP722 (Huang et al. 2007), DSDP231 (Feakins et al. 2013, Liddy et al. 2016) and ODP966-967 (Rose et al. 2016, Lupien et al. 2023). b) Desert pollen at site DSDP231 (Bonnefille 2010). c)  $\delta^{13}\text{C}_{\text{leaf wax}}$  at sites ODP659 and MD03-2705 (Kuechler et al. 2013, 2018, O'Mara et al. 2022).  $\delta^{13}\text{C}_{\text{soil carbonate}}$  from continental eastern Africa (Levin 2015 and references therein). e)  $\delta^{13}\text{C}_{\text{leaf wax}}$  at site ODP1081 (Rubelke et al. 2023). f) Desert pollen at site ODP1081 and 1082 (Dupont et al. 2005, Hoetzel et al. 2015). [Locations of marine sediment cores are visible on Figure 8.](#)

1557  
1558  
1559  
1560  
1561  
1562  
1563  
1564  
1565  
1566  
1567  
1568  
1569  
1570  
1571  
1572  
1573

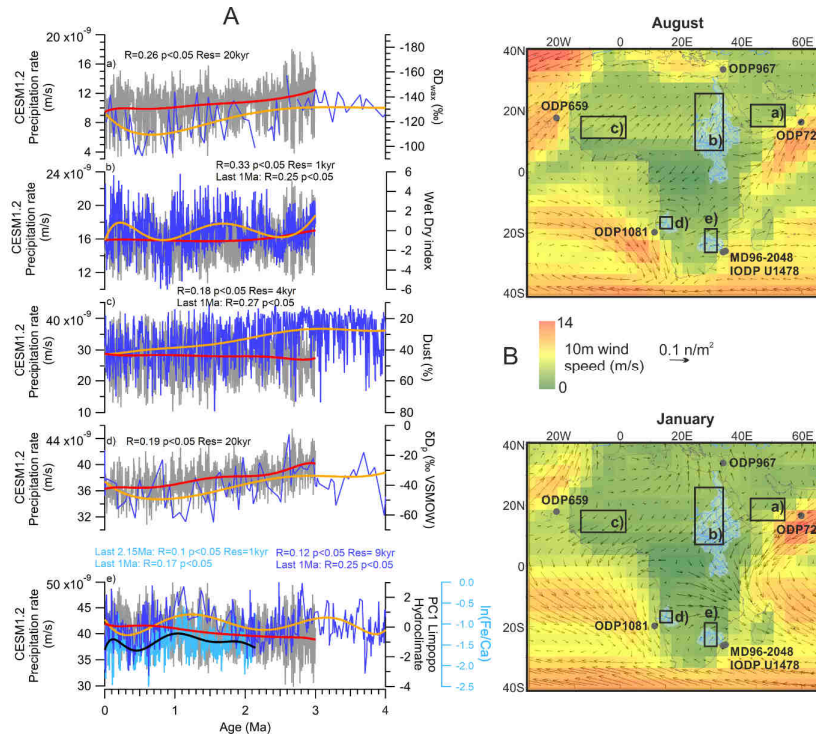


1574 Figure 10: African hominin species habitat suitability (results based on Timmermann et al.  
1575 2022). Species distribution calculated from a Mahalanobis distance model with coloured  
1576 circles represent the locations of fossils and/or archaeological artefacts associated with the  
1577 hominin groups. The time-averaged habitat suitability covering the period of respective  
1578 hominin presence can be interpreted in terms of probability, with values ranging from 0  
1579 (habitat unsuitable) to 1 (habitat extremely suitable) (Timmermann et al. 2022).

1580  
1581  
1582  
1583  
1584  
1585  
1586  
1587  
1588



1589  
 1590  
 1591  
 1592  
 1593  
 1594  
 1595  
 1596  
 1597  
 1598  
 1599  
 1600  
 1601



1602 Figure 11: Data-model comparison for African hydroclimate over the last 3Myr. A. Data in a)  
 1603 to e) are similar to Figure 6 a) to e), except the  $\ln(\text{Fe}/\text{Ca})$  hydroclimate record in e) (Caley et  
 1604 al. 2018). CESM1.2 annual simulated precipitation in a) to e) extracted from regions indicated  
 1605 by black frames in B. Polynomial fit (8th degree) documented in orange and red to  
 1606 demonstrate long-term trends and fluctuations in data and model respectively. The correlation  
 1607 coefficient (R) and corresponding significance (p) between data and model for specific time  
 1608 periods and resolution are shown. B. Wind speed at 10m and vectors of zonal and meridional  
 1609 surface wind stress averaged over the last 3Myr in the CESM1.2 simulation (Timmermann et  
 1610 al. 2022, Yun et al. 2023) for August (top) and January (down). Black frames denote the  
 1611 regions used for model results extraction and comparison in A.a) to e). These regions were  
 1612 defined as source regions of sedimentary materials transported to the studied marine cores by  
 1613 winds and river on the basis of present day river catchments and simulated mean wind speed  
 1614 and patterns over the last 3Myr in B.

1615  
 1616  
 1617  
 1618  
 1619  
 1620  
 1621  
 1622  
 1623

1624  
1625  
1626  
1627  
1628  
1629  
1630  
1631  
1632  
1633  
1634  
1635  
1636  
1637  
1638  
1639  
1640  
1641

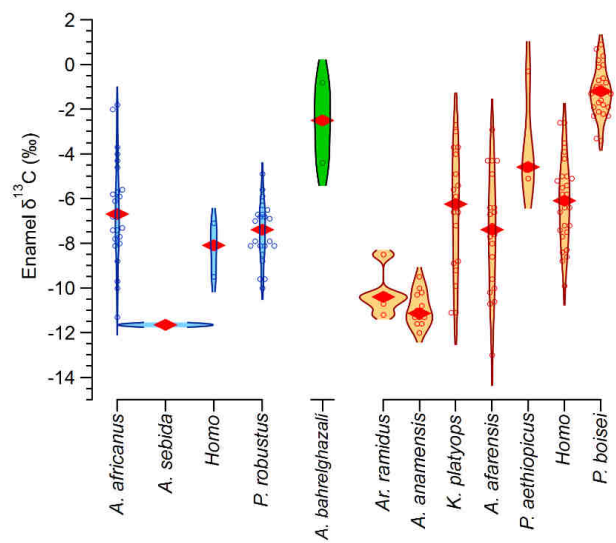


Figure 12: Enamel  $\delta^{13}\text{C}$  (representative of diets) of early hominin taxa from southern Africa (blue), central Africa (green) and eastern Africa (orange) arranged from oldest to youngest temporal periods/fossils for each regional group of African hominins (data from Sponheimer et al. 2013). Violin plots with the median values (red dots) are indicated.